Annales Societatis Geologorum Poloniae (2014), vol. 84: 259–279.

EARLY BADENIAN TRANSGRESSION ON THE OUTER FLANK OF WESTERN CARPATHIAN FOREDEEP, HLUCHOV AREA, CZECH REPUBLIC

Šárka HLADILOVÁ[1], Slavomír NEHYBA[2], Kamil ZÁGORŠEK[3], Pavla TOMANOVÁ PETROVÁ[4], Maria Aleksandra BITNER[5] & Attila DEMENY[6]

[1] *Department of Biology, Faculty of Education, Palacky University, Purkrabská 2, 771 46 Olomouc, Czech Republic; e-mail: sarka.hladilova@upol.cz*
[2] *Institute of Geological Sciences, Faculty of Science, Masaryk University, Kotlářská 2, 611 37 Brno, Czech Republic; e-mail: slavek@sci.muni.cz*
[3] *Department of Geography, Technical University of Liberec, Studentská 2, 461 17 Liberec, Czech Republic; e-mail: kamil.zagorsek@gmail.com*
[4] *Czech Geological Survey, Leitnerova 22, 658 69 Brno, Czech Republic; e-mail: pavla.petrova@geology.cz*
[5] *Institute of Paleobiology, Polish Academy of Sciences, Twarda 51/55, 00-818 Warszawa, Poland; e-mail: bitner@twarda.pan.pl*
[6] *Institute for Geological and Geochemical Research, RCSAES, Hungarian Academy of Sciences, Budaorsi ut 45, 1112 Budapest, Hungary; e-mail: demeny@geochem.hu*

Hladilová, Š., Nehyba, S., Zágoršek, K., Tomanová Petrová, P., Bitner, M. A. & Demeny, A., 2014. Early Badenian transgression on the outer flank of Western Carpathian Foredeep, Hluchov area, Czech Republic. *Annales Societatis Geologorum Poloniae*, 84: 259–279.

Abstract: This multidisciplinary study, based on borehole cores from the Hluchov area in Czech Republic, documents an early Badenian marine transgression on the outer flank of the Western Carpathian Foredeep. The shallow-marine deposits represent coastal transgression over a terrestrial topography of weathered pre-Cenozoic bedrock. The lower facies association (FA1) consists of siliciclastic sediment derived from local substrate erosion. Facies indicate a wave-dominated environment with unstable bottom, variable rate of sediment supply and an incremental rise of relative sea level. The upper facies association (FA2) consists of carbonates indicating a major landward shift of shoreline, decline in siliciclastic input and further sea-level rise. The succession represents a transgressive to highstand systems tract.

The maximum flooding surface, *ca*. 1 m above the FA1/FA2 boundary, is signified by an anomalous decrease in K and Th, an increased Th/K ratio and highest U concentration. The heavy-mineral assemblages in FA1 confirm local sediment provenance, whereas those in FA2 indicate broader sediment derivation, including volcanic component from contemporaneous rhyolitic to rhyodacitic eruptions. The deposits contain a wide range of marine fauna, with the foraminifers and molluscs indicating an early Badenian age. Molluscs, bryozoans and echinoderms indicate a normal-salinity environment with a decreasing hydraulic energy. Foraminifers indicate salinity fluctuations in the lowest part of the succession. The isotopic composition of mollusc shells shows marked inter-species differences and a general negative shift in the $\delta^{13}C$ and $\delta^{18}O$ values, indicating diagenetic alteration. The impact of diagenetic processes appears to have been controlled by sedimentary facies. The highly negative $\delta^{13}C$ and $\delta^{18}O$ values correspond to sediment layers with the highest Th/K ratios and hence low clay content. Sediment permeability was thus probably crucial in controlling the differential circulation and impact of diagenetic fluids.

Key words: Carpathian Foredeep, borehole cores, early Badenian, marine transgression, sedimentology, palaeontology, geochemistry.

Manuscript received 11 January 2014, accepted 13 November 2014

INTRODUCTION

Sedimentation at the cratonward margins of peripheral foreland basins is generally controlled by interplay of tectonism, eustasy and craton-derived sediment supply (Flemings and Jordan, 1989; Burbank and Beck, 1991; Johnson and Beaumont, 1995; Sinclair, 1997). The foredeep and forebulge morphology depends upon the flexural rigidity and tectonic deformation style of the foreland lithospheric plate, while the forebulge accommodation is modulated further by eustatic sea-level changes and craton sediment yield (Royden and Burchfiel, 1989; Royden, 1993; Matenco *et al.*, 2010).

The interplay and relative role of these controlling factors are analysed in the present case study, which docu-

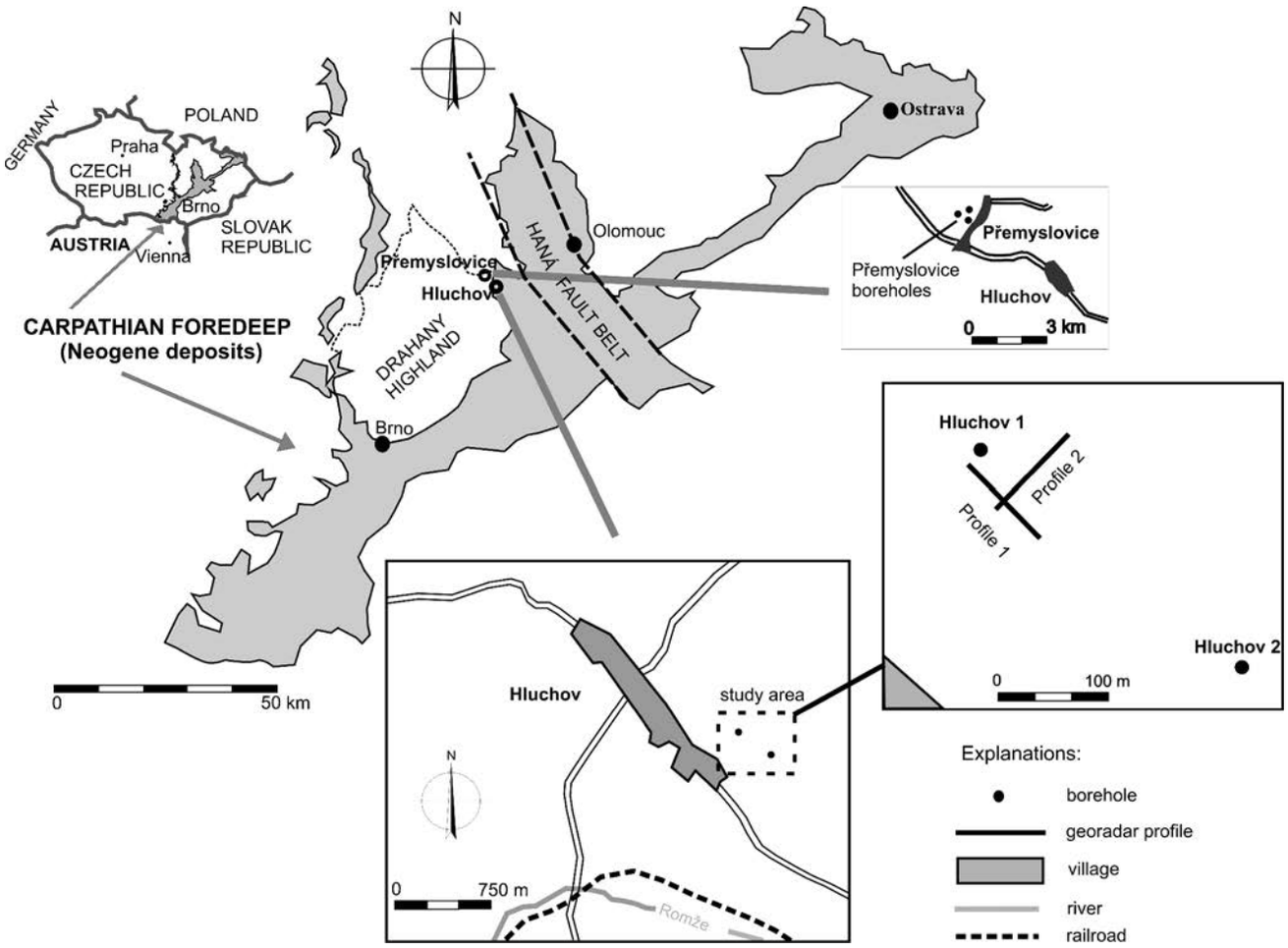

Fig. 1. Geographic location of the Neogene Western Carpathian Foredeep and the Hluchov boreholes (Hl-1 and Hl-2) and georadar profiles. Indicated also is the location of adjacent boreholes near Přemyslovice.

ments an early Badenian marine transgression on the basinward forebulge flank of the Western Carpathian Foredeep. The reported new evidence from borehole cores and georadar sections near Hluchov in central Moravia, Czech Republic (Fig. 1), combines sedimentological facies analysis with palaeontological and geochemical data to reconstruct the circumstances and environmental history of this transgression, which drowned the denudated subaerial peripheral bulge of the basin. The study as a whole contributes to a better understanding of the Neogene palaeogeographic development in Western Carpathian Foredeep, while also demonstrating the range of sedimentological, palaeontological and geochemical signatures of a major marine transgression on the low-relief peripheral bulge of a foredeep basin.

GEOLOGICAL SETTING

The pre-Neogene bedrock in the study area consists of the Culmian Lower Carboniferous (late Visean Myslejovice Fm), which is cropping out in the Drahany Highland (Fig. 1; Mísař *et al.,* 1983) and covers Precambrian crystalline basement. The Culmian clastic deposits are interbedded greywackes, siltstones and shales (Müller *et al.,* 2000).

The overlying Neogene deposits belong to the basin-fill of the Carpathian Foredeep. The foredeep formed as a peripheral foreland basin due to the tectonic emplacement and crustal loading of the Carpathian orogen onto the margin of the Bohemian Massif. Sedimentation in this sector of the foredeep commenced in the Egerian to early Eggenburgian and continued in the late Badenian. In the early middle Miocene, the basin geometry was reorganised by the northward (NW- to NNW-oriented) structural contraction of the Carpathian orogenic wedge (Nehyba and Šikula, 2007). The reactivation of NW-trending faults as the Haná Fault Belt (Fig. 1) played an important role in reshaping the topographic relief of the basin passive margin and changing its accommodation space. The fault-related high Neogene relief included narrow depressions and intrabasinal highs oriented at a high angle to the basin axial zone (Zapletal, 2004).

The oldest Neogene marine deposits in the broad surroundings of the study area are of Karpatian age, but their occurrences are rare (Vysloužil, 1981; Bubík and Dvořák, 1996). The basin-fill consists mainly of the early Badenian deposits, which commonly overlie directly the pre-Cenozoic bedrock. The greatest thickness of these deposits (more than 100 m) is known from the Prostějov and Lutín depressions to the east of the present study area. Numerous isolated relics of

Neogene deposits in the Drahany Highland (Fig. 1) represent an extension of the Prostějov depression towards the NW (Kalabis, 1961; Novák, 1975; Jašková, 1998; Zapletal *et al.*, 2001; Zapletal, 2004). New stratigraphic evidence comes from two cored shallow boreholes drilled recently near the village of Hluchov (Fig. 1), referred to as borehole Hl-1 (GPS location 49°32.322'N and 017°00.504'E, 377 m a.s.l.) and borehole Hl-2 (GPS location 49°32.914'N and 016°59.204'E, 341 m a.s.l.). Only some preliminary information from these boreholes has thus far been published (Zágoršek *et al.*, 2010; Nehyba and Jašková, 2012), and the aim of the present paper is to review and summarize results of a detailed sedimentological, palaeontological and geochemical analysis of the borehole cores. The study contributes to a better understanding of the history of early Badenian transgression in this part of the Carpathian Foredeep.

METHODS

A combination of sieving and laser methods was used for grain-size analysis. A Retch AS 200 wet-sieving machine was used to analyse coarse sediment fraction (0.063–4 mm) and a Cilas 1064 laser diffraction granulometer to analyse finer fraction (0.0004–0.5 mm). Ultrasonic dispersion, distillate water and washing in sodium polyphosphate were used prior to the grain-size analyses to avoid particle flocculation. The average grain size is given as a graphic mean (Mz) and the sediment sorting as the grain size standard deviation (σI) (Folk and Ward, 1957). The shape and roundness of the coarsest grains (4 mm) were estimated visually using the method of Powers (1982). Heavy minerals were studied in the grain-size fraction of 0.063–0.125 mm. The composition of selected heavy minerals was determined using a Cameca SX 100 electron microprobe at the Joint Laboratory of Electron Microscopy and Microanalyses of the Masaryk University and the Czech Geological Survey in Brno. Sedimentary facies analysis follows the sedimentological methodology outlined by Tucker (1995), Walker and James (1992) and Nemec (2005). The Paratethyan regional stratigraphic stages are according to Hilgen *et al.* (2012).

Ground-penetrating radar (GPR) survey was conducted with the use of Pulse Ekko Pro radar (manufactured by the Canadian Sensor & Software Ltd.) at 50-MHz frequency, an antenna distance of 3 m and measurement interval of 0.5 m. Acme Analytical Laboratories Ltd. (Vancouver) conducted chemical analyses of selected samples using standard analytical methods. The gamma-ray spectra (GRS) were measured by a GR-320 enviSPEC laboratory spectrometer with a 3×3 inch NaI(Tl) scintillation detector (Canadian Exploranium Ltd. product). Counts per second in selected energy windows were directly converted to concentrations of K (%), U (ppm) and Th (ppm). One measurement with a 30-minute count time was performed for each measured sample (300 g minimum weight).

Palaeontological study of bryozoans was based on 37 samples from the borehole Hl-1 core and 25 samples from the borehole Hl-2 core. The samples were washed in running water using sieves with 2, 0.9 and 0.063 mm mesh. Detailed SEM study of uncoated specimens was performed with a Hitachi S3700N microscope. The whole material is now stored at the National Museum in Prague.

Analysis of foraminiferal assemblages was based on 28 samples from borehole Hl-1, using sample-wash residua and a NIKON binocular microscope. Groups of shallow-marine warm- and cold-water foraminifers were interpreted according to the palaeoecological studies of Ingle (1980), Hudáčková (1995), Harloff and Mackensen (1997), Rögl and Spezzaferri (2003) and Murray (2006). The Paratethyan foraminifer biostratigraphy is based on Cicha *et al.* (1998).

Molluscan fauna was studied from the sample-wash residua (28 samples from borehole Hl-1 and 17 samples from borehole Hl-2), using NIKON and SZP 11-BH binocular microscopes and photographed with the OLYMPUS camera and SEM JEOL JSM-649 OLV at the Institute of Geological Sciences, Masaryk University.

Brachiopods were found in 13 of the 37 samples taken from borehole Hl-1, with a total of 51 specimens (47 articulated, 3 ventral and one dorsal valve).

Shells of 4 mollusc species (*Crassadoma multistriata, Flexopecten scissus, Chlamys trilirata,* Pectinidae indet.) represented by 34 specimens (22 from borehole Hl-1 and 12 from borehole Hl-2) have been analysed for stable O and C isotopes at the Institute for Geological and Geochemical Research, RCAES, Hungarian Academy of Sciences (Budapest). Carbon and oxygen isotope composition of calcite was determined with the method of acid digestion of the carbonate samples (for analytical details, see Spötl and Vennemann, 2003). These isotope analyses were conducted using automated GASBENCH equipment attached to a Finnigan Thermo delta plus XP mass spectrometer. The compositions are given as $\delta^{13}C$ and $\delta^{18}O$ values (in ‰) relative to the international standard V-PDB, according to the equation:

$$\delta = (R_{sample}/R_{standard} - 1) \times 1000$$

where R is the $^{13}C/^{12}C$ or $^{18}O/^{16}O$ ratio in the sample and in the standard, respectively. Multiple analyses of standards indicated analytical precision better than ±0.15‰. For comparison, the isotopic data from the Hluchov boreholes were supplemented with analogical data from 13 specimens of 3 mollusc species (*Crassadoma multistriata, Flexopecten scissus, Aequipecten macrotis*) from the Přemyslovice boreholes (Fig. 1): 4 specimens from borehole PY-5, 8 specimens from PY-6 and 1 specimen from PY-7.

RESULTS

Georadar survey

Two perpendicular georadar profiles were taken in the vicinity of borehole Hl-1 (Fig. 1) with the aim to determine the topography of pre-Neogene bedrock and recognize the shape of the lower Badenian body of deposits. These geophysical profiles indicate that the lower Badenian is about 20 m thick and rests on a slightly undulated surface of pre-Neogene bedrock. The bedrock is a thick section (about 10 m) of the weathered sedimentary rocks of Myslejovice

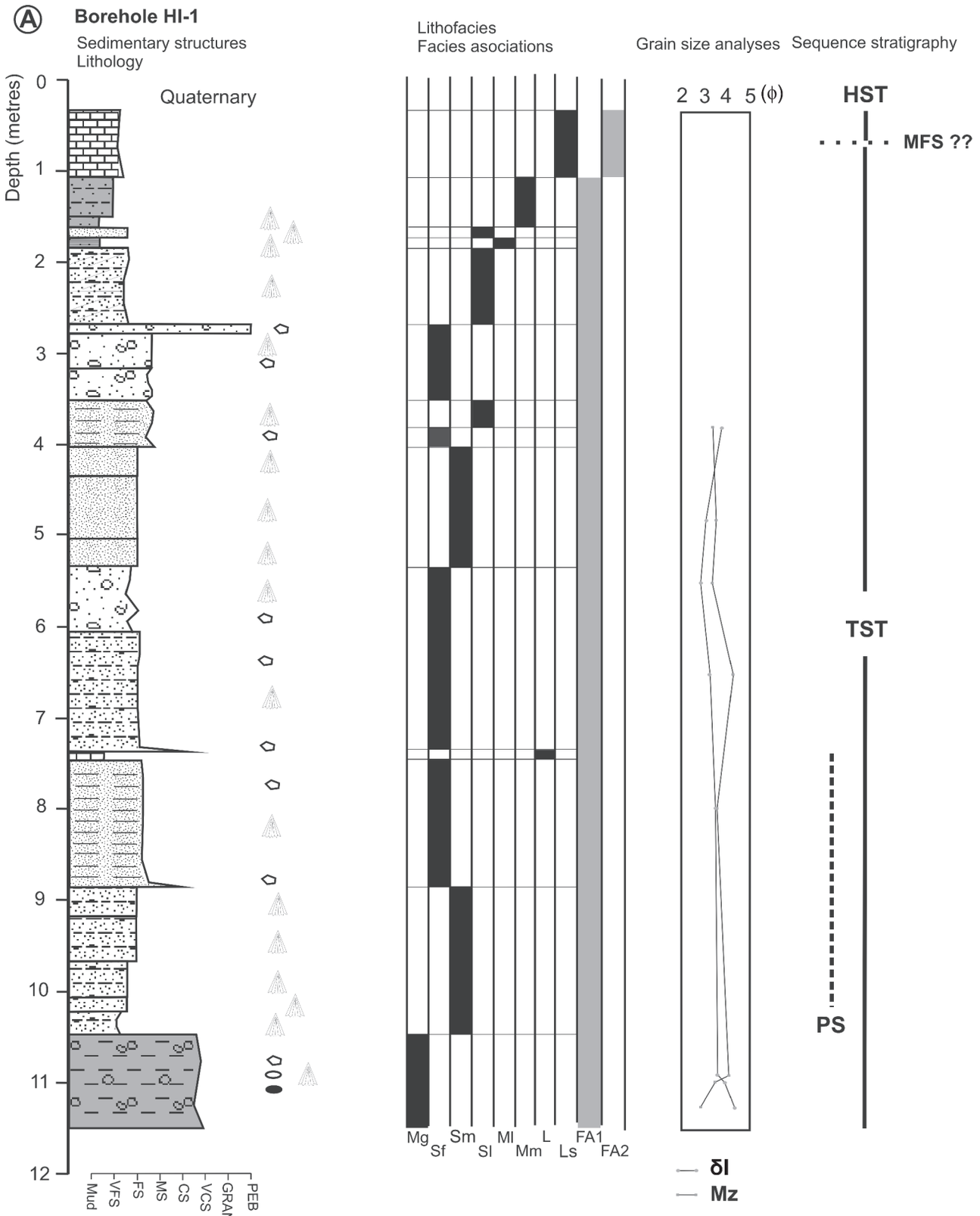

Fig. 2. Sedimentological core logs of the Hluchov boreholes Hl-1 (**A**) and Hl-2 (**B**). The logs include palaeontological data and show the stratigraphic distribution of sedimentary facies (letter code as in Table 1), distinction of facies associations (FA1 and FA2), plot of mean grain size and sequence-stratigraphic interpretation (letter symbols explained in legend).

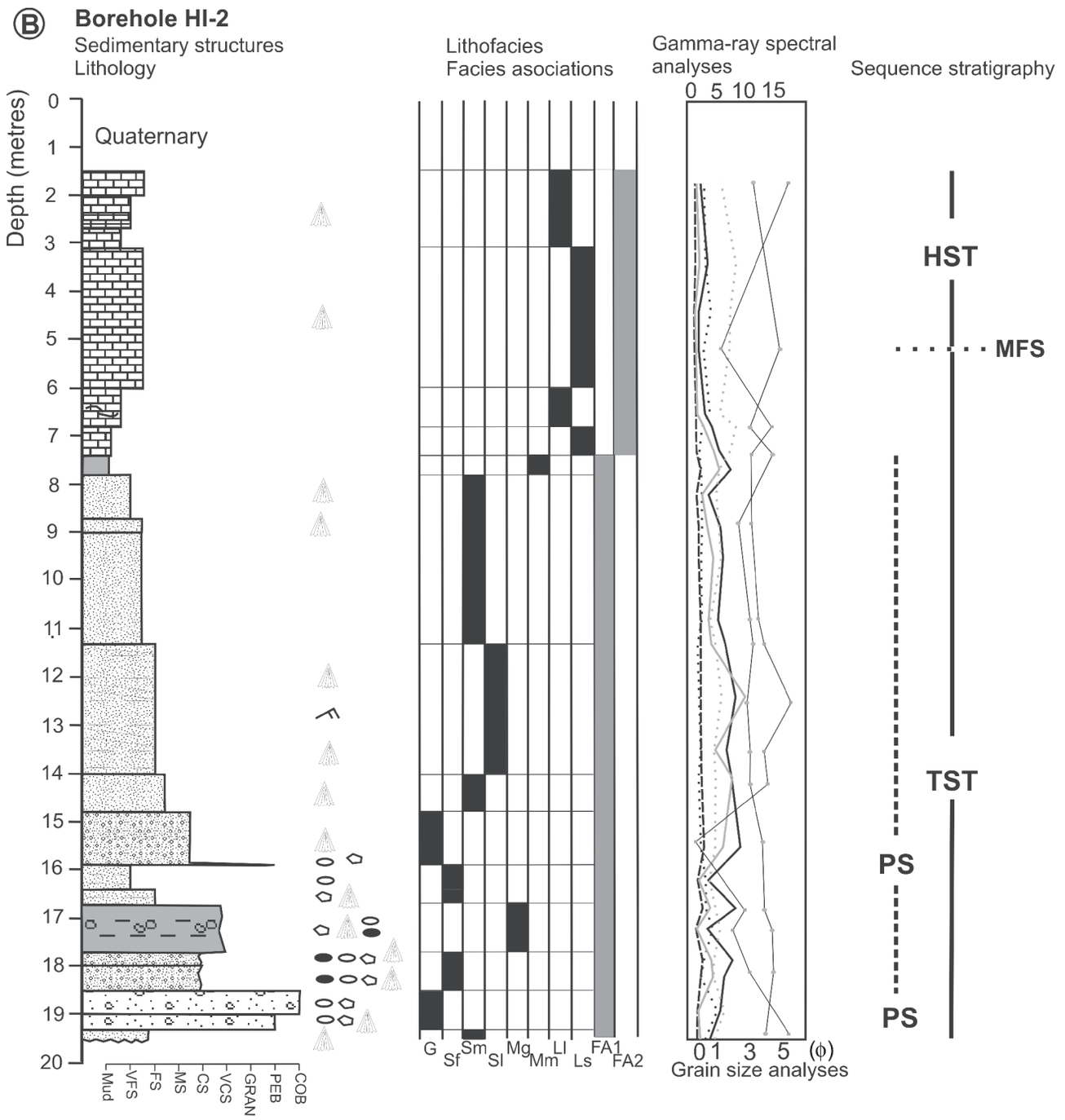

Log legend

clay / mud
sandy mud with pebbles
sand
sandy gravel
sandy limestone
planar lamination
ripple cross-lamination
angular clasts
rounded clasts
clayey intraclasts
shells (molluscs)
FA facies association
PS parasequence
TST transgressive systems tract
HST highstand systems tract
MFS maximum flooding surface
δI
Mz
Th (ppm)
U (ppm)
K (%)
Th/U
Th/K

Table 1

Descriptive summary list of early Badenian lithofacies distinguished in the Hluchov boreholes Hl-1 and Hl-2. Mz is the mean grain size and σI is grain-size standard deviation (sorting)

Facies symbol	Description
G	Gravel, clast supported to matrix supported (matrix of muddy sand). Rounded to angular pebbles, max. clast up to 15 cm in diameter, usually about 3 cm. Largest clasts along the base and top of the bed, sandy matrix, poorly sorted, shell debris. Mz = –0.23 ϕ, σI = 3.7 ϕ. Facies represents 4.7% of the succession.
Sf	Reddish green, green-grey, yellow green, whitish or brownish mottled, poorly sorted, fine, fine to medium sand, admixture of pebbles (up to 3 cm in diameter), shell debris (oysters). Varied content of mud, occasional flasers of green mudstone up to 2 cm thick, sharp base with clasts, massive or irregularly bedded. Mz = 3.4–4.3 ϕ, σI = 3.7–4.4 ϕ. Facies represents 27.3% of the succession.
Sm	Light yellow-brown, light grey, green grey to whitish fine to very fine massive sand, poorly sorted due to admixture of mud, significant content of shell debris. Granules and small pebbles are very rare. Mz = 3.5–5.3 ϕ, σI = 3.0–4.0 ϕ. Facies represents 27.7% of the succession.
Sl	Light yellow green, whitish yellow fine to very fine sand, relative better sorted, planar lamination or ripple bedding. Rare shell debris, very rare subangular small pebbles up to 2 cm (along the base of the bed). Mz = 3.4–5.5 ϕ, σI = 2.8–3.1 ϕ. Facies represents 13.6% of the succession.
Mg	Light yellow grey, red to brown mottled, gravely sandy mud. Rounded to angular pebbles, max. 5 cm in diameter. Intraclasts of reddish mudstone, shell debris (oysters). Mz = 2.9–4.1 ϕ, σI = 3.6–4.4 ϕ. Sometimes alternation of light grey muddy sand with planar lamination, rare shell debris and pebbles and thin irregular beds (thickness about 2 cm) of green massive mudstone (up to 2 cm). Facies represents 3.0% of the succession.
Ml	Light grey-green, whitish grey, whitish green to green, reddish mottled, muddy sand to sandy mud with shell debris (oysters). Crude planar stratification. Facies represents 0.5% of the succession.
Mm	Whitish grey to light grey massive calcareous mud. Low admixture of fine sand. 3.3% of the succession.
L	Whitish sandy limestone, lumachelle of shells. Facies represents 0.3% of the succession.
Ls	Whitish green-gray fine to very fine sand, calcareous sand to sandy limestone, massive. Relatively good sorted. Facies represents 13.0% of the succession.
Ll	Whitish grey, light grey to white micritic limestone, planar lamination, small admixture of allochems (shells), rare thin clay laminae. Mz = 4.3–5.6 ϕ, σI = 3.0–3.1 ϕ. Facies represents 6.6% of the succession.

Fm (upper Visean). Internal bedding reflectors in the lower Badenian indicate a generally planar (aggradational) architecture with a slight basinward progradation approximately towards the south-east.

Sedimentary geology and gamma-ray spectral analyses

Lithofacies were defined on the basis of sediment grain size, rare preserved sedimentary structures and petrology (Table 1). On the basis of their stratigraphic distribution (Fig. 2) and broad georadar architecture, the ten lithofacies have been grouped further into two facies associations (*sensu* Reading, 1996) – a lower and an upper one (Fig. 2).

Lower facies association

The lower facies association (FA1) is 10–12 m thick (base not reached by wells) and consists of 6 lithofacies (G, Sf, Sm, Sl, Mg, Mm, Ml and sporadic L; Table 1) organized into two fining-upwards cyclothems (see Fig. 2).

The lithology of gravel clasts (size 4 mm) indicates a wide range of surrounding bedrock components. The largest clasts are pebbles of Culmian greywackes, shales and siltstones, which often dominate (8.9–63.9%) and are typically spherical, discoidal or bladed in shape. Pebbles of milky quartz form 2.8–19.1%, whereas the remaining few per cent consists of metavolcanites, quartzites, gneisses, phyllites, cherts, quartzose sandstones, orthoquartzite (bright "sunstone") and quartz-feldspar aggregates. The clasts are mainly subangular to subrounded, less commonly rounded. Small oval depressions on pebble surfaces show mollusc remnants, reflecting the attachment of these shells to the large, least mobile sediment grains on sea floor. The content of gravel and the percentage of Culmian rock clasts are highest in the basal part of FA1, where even angular to subangular cobbles of wackes (up to 15 cm in size) occur.

The transparent heavy-mineral assemblage in FA1 is dominated by zircon (30.3–56%) and garnet (12–17.4%), with significant contents of disthene (5.4–15.2%) and apatite (4.6–13.0%) in only some samples. The occurrence of other transparent heavy minerals (tourmaline, staurolite, rutile, titanite, epidote, spinel, andalusite, anatase) amounts to only a few percent. The high content of most stable minerals and the ZTR index of 40.9–62.4% are remarkable, highest at the base of FA1. Zircons grains are mainly rounded (47%) and subhedral in shape (29%), less commonly euhedral (24%), with crystal planes preserved in 58% of the grains. Less common are zoned zircons (24%) and grains with older cores (18%). The majority (93%) of zircons contain inclusions. The mean value of zircon elongation is 2.0, with a maximum of 2.9. A typological analysis of zircon population (Pupin, 1980), here based on 47 grains, shows that the majority (66%) of the euhedral zircons belong to subtypes S18, S19, S23 and S24; subtypes S8, S9, S17, S20, S22 and S25 are less common.

The gamma-ray spectral (GRS) logs show a considerable degree of vertical variability in FA1 (Fig. 2). These siliciclatic deposits have relatively high concentrations of K (∅ 1.3%) and Th (∅ 6.2 ppm) and a high Th/U ratio (∅ 3.8), but a lower concentration of U (∅ 2.1 ppm) and a higher Th/K ratio (∅ 4.8). They show significant variation in Th (standard deviation SD 2.1), K (SD 0.5), U (SD 1.0) and also the Th/U ratio (SD 2.4). Statistical correlation between the bulk

gamma-ray intensity (dose rate) and the K, Th and U individual concentrations indicates that the main contribution to the gamma-ray signal comes from Th (linear regression coefficient r = 0.64) and K (r = 0.59), and much less from U (r = 0.14). The K and Th concentrations show an almost perfect correlation (r = 0.91). On the other hand, there is a negative correlation between K and U (r = –0.48) and between Th and U (r = –0.52). The correlation between U and clay content is very low (r = 0.13), and there is a negative correlation between the clay content and both K (r = –0.66) and Th (r = –0.45), which indicates that the radioactive elements occur mainly in the sand, rather than mud fraction.

The vertical variability in GRS logs is consistent with the changes in lithofacies and partly also sediment grain size (Fig. 2). The mudstone facies Mg and Ml (Table 1) have a relatively low concentration of K (0.5–1.8%), but higher concentration of Th (2.9–8.5 ppm) and U (1.6–4.0 ppm). Their Th/U ratio varies greatly (0.7–4.0), whereas the Th/K ratio (4.1–5.6) is relatively stable. Sandstone facies show high variation in the contents of radioactive elements. The sandstone facies Sm (Table 1) has a relatively low concentration of Th (3.2–7.9 ppm) and concentration of K (0.7–1.7%) similar to that in facies Sl, but its concentration of U (1.1–2.4 ppm) is higher than the latter facies. Facies Sl shows concentrations of K of 1.4–1.6%, Th of 6.6–8.7 ppm and U of 0.8–1.7 ppm. The Th/U ratio in facies Sm (1.3–7.0) is lower than in facies Sl (3.7–10.7), whereas the Th/K ratio in the former facies (3.5–5.8) is comparable to that the latter facies (4.3–5.8).

The FA1/FA2 boundary shows a marked drop in the K and Th concentrations and the Th/U ratio, but a rise in the Th/K ratio. Higher U concentrations occur at around 1 m above the boundary. This change in radioactive element contents may indicate a significant decrease in terrestrial sediment input due to a landward shoreline shift (i.e., marine flooding).

Upper facies association

The upper facies association (FA2 in Fig. 2) consists of lithofacies Ll and Ls (Table 1). It is calcareous, finer- grained and lacking gravel. The assemblage of transparent heavy minerals is dominated by garnet (30–35%), disthene (17–28%) and epidote (13–14%), with a variable admixture of apatite (5–17.2%) and staurolite (3.8–10.3%). The relative amount of other transparent heavy minerals (zircon, tourmaline, zoisite, spinel) is only a few per cent. The content of most stable minerals is low and the ZTR index varies between 3.4 and 8.3%. Zircons have predominantly euhedral (41.2%) or subhedral shape (35.3%), with rounded shapes less common (17.5%). Crystal planes are preserved in 58.8% of zircon grains. Zoned zircons are uncommon (8.8%) and zircons with older cores are rare (2.8%). Most zircons (97.2%) contain inclusions. Typologically, the majority of euhedral zircons (68.2%) represent subtypes P1, P2 and P3 (*sensu* Pupin, 1980), with subtypes S13, S14, S17, S20 and S23 less common. The value of zircon elongation averages 2.9 and exceeds 3.0 for 33.3% and 4.0 for 16.7% of grains.

There is no recognizable difference in garnet chemistry between FA2 and FA1. Almandine garnets predominate, with pyrope-almandines (73.3%), spessartine-pyrope-almandines (13.3%), grossular-almandines (6.6%), grossular-pyrope-almandines (3.3%) and spessartine-almandines (3.3%).

Notable is the subordinate presence of rutile, one of the most stable heavy minerals, which is known to derive primarily from medium- to high-grade metamorphic rocks or to be recycled from older clastic sediments. Although the signature of multiple metamorphic cycles in rutile is disputed (Stendal *et al*., 2006; Meinhold *et al*., 2008), this mineral is attractive for provenance analysis (Force, 1980; Zack *et al*., 2004; Triebold *et al*., 2005). In the present case, the concentration of the main diagnostic elements (Fe, Nb, Cr and Zr) varies greatly. The majority (88.5%) of rutiles show Fe concentration of above 1000 ppm. The concentration range of Nb is 199–2967 ppm (mean 902 ppm), of Cr is 10–869 ppm (mean 450 ppm), and of Zr is 51–1784 ppm (mean 837 ppm). The value of logCr/Nb is negative in 76.9% of the samples.

Gamma-ray spectral logs (Fig. 2) show the carbonate facies association FA2 to have very low mean concentrations of K (∅ 0.4%) and Th (∅ 2.6 ppm), but a fairly high concentration of U (∅ 2.4 ppm). The concentration variability is relatively low for K (standard deviation SD = 0.2) and U (SD = 0.8), but high for Th (SD = 1.4). The bulk gamma-ray intensity (dose rate) correlates well with the content of U (r = 0.65), but poorly with the content of K (r = 0.13) and particularly Th (r = –0.09). Again, there is an almost perfect correlation between these latter two elements (r = 0.96), a weak correlation between U and Th (r = 0.33), and a negative correlation between K and U (r = –0.54) and between Th and U (r = –0.65). The clay content shows negative correlation with both K (r = –0.44) and Th (r = –0.53), which again indicates that the main part of the radioactive elements occurs in sand fraction, rather than in mud. The lowest Th/U ratio, *ca.* 4.4 m above the base of FA2, corresponds to the lowest concentrations of K and Th and the highest of U, which may indicate conditions of maximum flooding (see Lüning *et al*., 2003; Doveton and Merriam, 2004; Halgedahl *et al.*, 2009).

The GRS logs of FA2 show less vertical variability, but seem to reflect lithofacies changes (Fig. 2). The carbonate facies Ll and Ls (Table 1) show relatively low concentration of K (0.2–0.6%) and Th (1.1–3.8 ppm), but a higher concentration of U (1.8–3.6 ppm). The Th/U ratio is low (0.3–2.1), whereas the Th/K ratio is relatively high (5.5–8.8). The anomalously low concentrations of K and Th in facies L reflect a significantly reduced admixture of terrigenous sediment (Langmuir and Herman, 1980). Facies L is also richer in uranium, relative to other radioactive elements, which is reflected in the low Th/U ratio and indicates high carbonate content (Berstad and Dypvik, 1982). The source of radioactive elements in FA2 is thus slightly different, but generally connected with sand fraction.

Palaeontological data

Foraminifera

Results of a systematic sampling of the core from borehole Hl-1 are listed in Table 2. The part of succession (depth

Table 2

List of Foraminifera species found at particular depths in the borehole core profile Hl-1 (see log in Fig. 2A)

Foraminifera: Taxa/Succession level (cm)	80	130	170	200	230	250	350	410	490	520	580	620	650	690	700	730	780	820	880	900	920	940	980	1000	1040	1080	1100	1150
Benthos																												
Ammonia beccarii (Linne)	1				1	1	1	1			1	1	1	1	1	1		1	1	1		1	1		1	1	1	
Ammonia viennensis (d`Orbigny)	1	1										1			1	1				1			1	1	1		1	
Ammonia tepida (Cushman)												1	1						1									
Ammonia sp.														1		1												
Amphicoryna badenensis (d`Orbigny)									1																			
Amphistegina haueriana Neugeboren							1																	1				
Amphistegina mammilla (Fichtel & Moll)							1																					
Amphistegina sp.								1																				
Asterigerinata planorbis (d`Orbigny)	1	1	1	1	1	1	1	1	1	1		1	1					1	1		1			1			1	1
Aubignyna perlucida (Heron-Allen & Earland)																			1				1	1	1			
Aubignyna sp.																		1										
Biapertorbis biaperturatus Pokorny																1												
Biapertorbis sp.			1	1	1	1	1	1	1	1	1	1	1	1	1													
Bolivina antiqua d`Orbigny							1			1		1	1	1		1					1					1		
Bolivina dilatata Reuss		1																										
Bolivina sp.						1			1																			
Cassidulina laevigata d`Orbigny		1																										
Cibicidoides ungerianus (d`Orbigny)																		1										
Cibicidoides sp.		1			1																							
Elphidium aculeatum (d`Orbigny)	1																											
Elphidium crispum (Linne)	1	1		1	1	1	1	1	1	1			1	1		1		1	1	1	1				1		1
Elphidium fichtelianum (d`Orbigny)	1	1	1	1	1	1			1	1	1	1		1	1	1					1	1		1	1	1		1
Elphidum flexuosum (d`Orbigny)	1	1	1	1	1	1	1	1	1	1	1	1	1	1	1	1		1	1	1	1	1	1					1
Elphidium cf. hauerinum (d`Orbigny)					1		1						1											1				
Elphidium sp.									1	1		1												1				1
Glandulina ovula d`Orbigny						1																						
Globulina gibba d`Orbigny	1	1		1	1		1	1	1					1		1				1				1	1	1		
Guttulina communis (d`Orbigny)				1	1										1													
Guttulina sp.						1																						
Hanzawaia boueana (d`Orbigny)	1	1	1	1	1	1	1	1	1		1	1	1		1	1			1	1			1		1			
Hanzawaia cf. *horčici* (Cicha & Zapletalová)		1																										
Hanzawaia sp.		1			1		1			1		1		1							1	1		1		1		
Hansenisca soldanii (d`Orbigny)			1			1			1																			
Heterolepa dutemplei (d`Orbigny)	1	1	1			1	1		1	1													1					

Tab. 2 cont.

Foraminifera: Taxa/Succession level (cm)	80	130	170	200	230	250	350	410	490	520	580	620	650	690	700	730	780	820	880	900	920	940	980	1000	1040	1080	1100	1150
Hoeglundina elegans (d`Orbigny)	1															1												
Laevidentalina elegans (d`Orbigny)															1									1				
Lagena striata (d`Orbigny)	1			1																								
Lenticulina cultrata (Montfort)		1	1		1	1					1																	
Lenticulina echinata (Soldani)		1	1																									
Lenticulina inornata (d`Orbigny)		1		1		1		1	1		1	1	1	1		1			1	1	1	1	1	1		1	1	
Lenticulina macrodisca (Reuss)			1	1								1	1		1								1	1	1			
Lenticulina melvilli (Cushman & Renz)			1			1					1																	
Lenticulina vortex (Fichtel & Moll)					1																							
Lenticulina sp.	1	1		1			1			1		1		1	1	1		1	1	1	1		1	1	1		1	
Melonis pompilioides (Fichtel & Moll)							1								1	1					1							
Neoponides schreibersi (d`Orbigny)	1														1				1				1	1				
Nonion commune (d`Orbigny)								1			1	1		1				1							1	1	
Pappina breviformis (Papp et Turnovsky)											1			1		1												
Pappina sp.													1											1				
Pararotalia aculeata (d`Orbigny)	1					1			1												1							
Pararotalia canui (Cushman)			1	1	1	1			1		1		1	1							1							
Pararotalia sp.		1					1	1				1											1	1			1	
Planularia sp.		1	1																									
Porosononion granosum (d`Orbigny)					1	1	1		1		1	1	1			1							1	1		1		
Pyramidulina raphanistrum (Linne)						1							1		1			1										
Quinqueloculina akneriana d`Orbigny														1														
Quinqueloculina haidingeri d`Orbigny	1	1																										
Quinqueloculina sp.	1		1			1																						
Reussella spinulosa (Reuss)	1	1	1	1	1	1						1		1		1			1		1			1				
Reussella sp.													1	1	1													
Semivulvulina pectinata (Reuss)		1																										
Siphonina sp.						1																						
Stilostomella verneuilli (d`Orbigny)			1																									
Textularia gramen d`Orbigny				1																								
Textularia pala Czjzek						1										1												
Textularia sp.						1																						
Triloculina gibba d`Orbigny				1																								
Triloculina sp.		1																										

Tab. 2 cont.

Foraminifera: Taxa/Succession level (cm)	80	130	170	200	230	250	350	410	490	520	580	620	650	690	700	730	780	820	880	900	920	940	980	1000	1040	1080	1100	1150
Uvigerina pygmoides Papp & Turnovsky															1													
Valvulineria complanata (d`Orbigny)																		1						1			1	
Plankton																												
Globigerina bulloides d`Orbigny														1		1												
Globigerina diplostoma Reuss													1															
Globigerina praebulloides Blow	1	1		1	1	1						1	1			1												
Globigerina tarchanensis Subbotina & Chutzieva															1					1		1	1					
Globigerina sp.						1							1		1						1							
Globigerinella regularis (d`Orbigny)											1		1		1	1												
Tenuitellinata angustiumbilicata (Bolli)						1																						

interval 11.50–10.40 m, Fig. 2A) contains sparse and low-diversity foraminiferal assemblages with numerous specimens of the *Ammonia* group accompanied by lenticulinas. Lenticulinas occur coupled with *Elphidium* div. sp. and *Asterigerinata planorbis* (d´Orb.) higher upwards in the succession (depth interval 9.80–5.80 m). The lenticulina tests are damaged and corroded, whereas the tests of other foraminifers inhabiting warm shallow water are well preserved, with conserved sculpture. No foraminifers were found in the washed residua from the core depth of 7.80 m (Fig. 2A). A change of the composition of foraminiferal assemblage is recognizable from the depth of 5.20 m upwards, with numerous well-preserved diversified elphidia (*Elphidium crispum, Elphidium fichtelianum, Elphidium flexuosum*, *Elphidium* cf. *hauerinum*) accompanied by such species as *Asterigerinata planorbis*, *Reussella spinulosa* and *Quinqueloculina* div. sp. The elphidia species indicate shallow water and possibly lagoonal conditions. Agglutinated foraminifers are rare in the whole profile. More abundant lenticulinas coupled with shallow-water taxa were found at the depth of 3.50 m. Typical warm shallow-water species occur in the uppermost interval of 0.80–2.50 m (Fig. 3H).

Bryozoa

The data on bryozoans from boreholes Hl-1 and Hl-2 are summarized in Table 3. In total, 33 bryozoan species have been identified, including 13 cyclostomatous and 20 cheilostomatous species. The dominant species belong to the *Ceriopora/Cellepora* and *Reteporella* groups (Fig. 3A–D). Erect colony growth forms predominate, with only 8 species from encrusting colonies.

Bryozoans occur uniformly throughout the profile, with 2 to 4 or occasionally 5 species in every sample. Exceptionally rich are samples from the upper part of the profile (depth interval 2.00–2.50 m in borehole Hl-1 and interval 1.20–1.80 m in borehole Hl-2, Fig. 2), which seem to represent a regional bryozoan event (*sensu* Zágoršek, 2010).

Apart from this apparent late bloom event, the low diversity of species indicates a marine environment hardly hospitable to bryozoans, which can be attributed to high water energy (notion supported by the dominance of reteporiform species), a high rate of sedimentation and/or deep oligotrophic water.

Brachiopoda

Samples from borehole HL-1 show that brachiopods are rare and of low diversity (Table 4), represented by micromorphic species *Argyrotheca bitnerae* Dulai, 2011, *Joania cordata* (Risso, 1826) and *Platidia* sp. (Fig. 4). *A. bitnerae* dominates, with 37 specimens found in 9 samples. Much less frequent are *J. cordata* (found in 6 samples) and *Platidia* sp. (found in 2 samples). A single sample usually yielded just one species. Two species were found in only two samples (from the core depths of 2.50 and 7.00 m; Fig. 2A) and three in just one sample (core depth 2.30 m), where also brachiopod specimens were most numerous.

Mollusca

The occurrence of molluscs in the cores from boreholes Hl-1 and Hl-2 is summarized in Table 5. Bivalves predominate and scaphopods are less frequent, whereas gastropods are absent. In borehole Hl-1 (Fig. 2A), bivalves occur throughout the profile and are most frequent at the depth interval of 9.40–5.80 m. Representatives of Pectinidae family and less frequent scaphopods occur throughout. Fragments of oyster shells predominate in the lower part of the profile. In borehole Hl-2 (Fig. 2B), bivalves are abundant only in the lower part of the profile (depth interval 19.50–13.50 m), where oysters dominate and pectinids are infrequent. Higher upwards, the amount of bivalves distinctly decreases, oysters are nearly absent and various pectinid species predominate. Scaphopods were found only at the core depth of 10.80 m. The most common bivalve species are *Crassadoma multistriata* Poli (1795), *Aequipecten* sp., *Macrochlamis* cf. *nodosiformis* (de Serres in Pusch, 1837) and *Neopycnodonte* sp. (Fig. 3E–G).

Other fossils

Other fossils (Table 6) include Echinodermata, which occur almost continuously in both profiles as the plates and

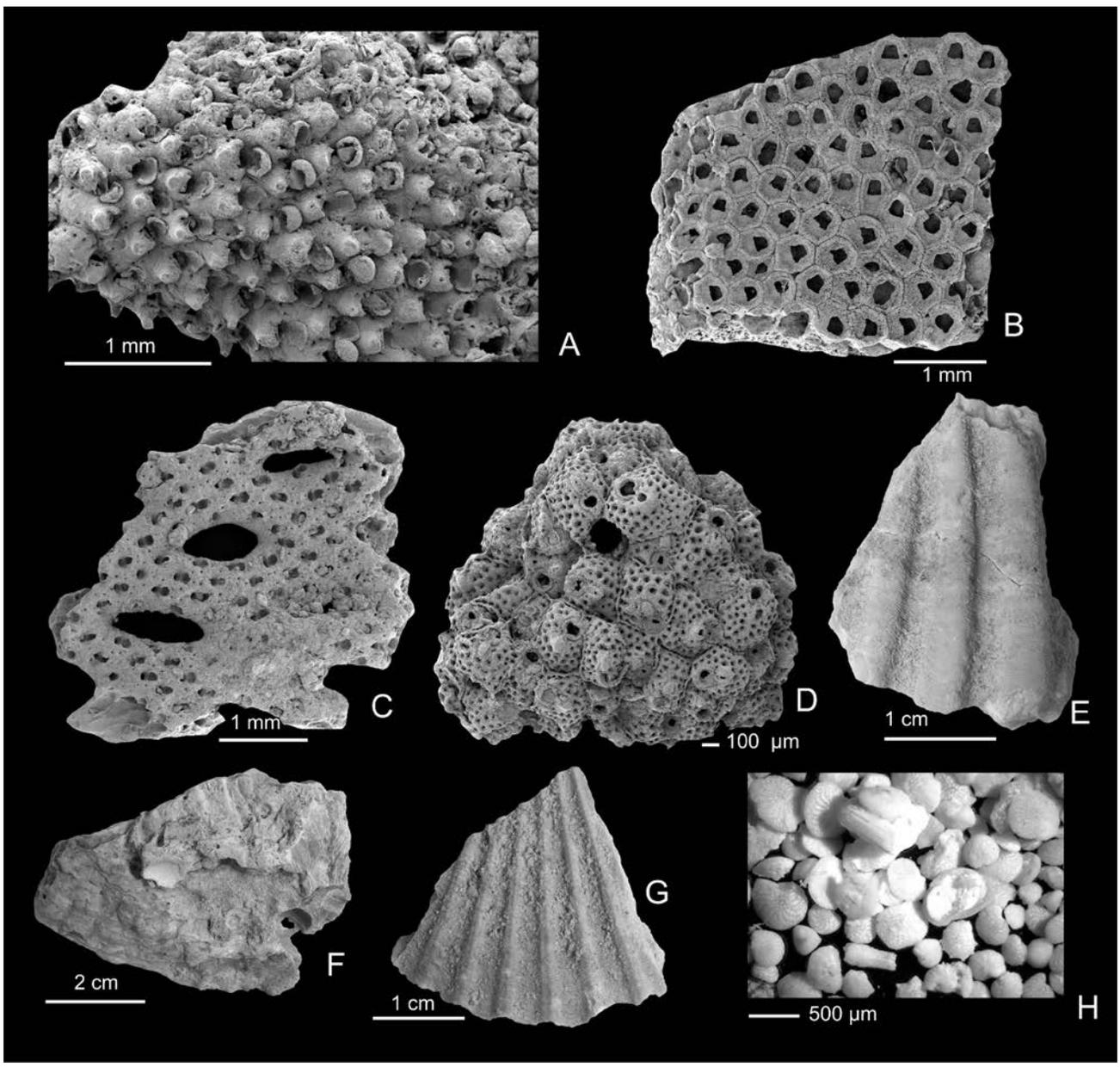

Fig. 3. Examples of Foraminifera, Bryozoa and Mollusca from the Hluchov boreholes Hl-1 and Hl-2. **A.** *Rhynchozoon monoceros* (Reuss, 1848); Hl-1, depth 1.80 m. **B.** *Onychocella angulosa* (Reuss, 1848); Hl-1, depth 1.80 m. **C.** *Reteporella hluchovensis* Zágoršek, 2010; Hl-1, depth 1.80 m. **D.** *Schizoporella dunkeri* (Reuss, 1848); Hl-1, depth 1.80 m. **E.** *Macrochlamis* sp., Hl-1, depth 7.30 m. **F.** Ostreidae, Hl-2, depth 17.20 m. **G.** *Pecten subarcuatus styriacus*, Hl-1, depth 1.30 m. **H.** Assemblage of foraminifers dominated by *Elphidium* sp., Hl-1, depth 0.80 m.

spines of echinoids and plates of asteroids and ophiuroids, and are particularly abundant at the depth interval of 5.20–0.80 m in borehole Hl-1 (Fig. 2A). Another important component of the palaeobiocoenoses are arthropods Cirripedia, which occur throughout the profiles and are conspicuously abundant in the upper part of borehole Hl-1 (depth 6.50–0.80 m) and middle part of borehole Hl-2 (depth 10.80–11.30 m), where they even prevail over bivalves. Serpulid tubes are common, but less frequent, and occasionally found are Teleostei teeth and otoliths. Exceptional is the occurrence of colonial corals in borehole Hl-1 (depth 10.40 m, Fig. 2A).

Isotopic composition of molluscs

Results of the isotopic analyses of mollusc shells from boreholes Hl-1 and Hl-2 are given in Tables 7 and 8. The $\delta^{18}O$ values range from –4.68‰ to –1.60‰ with a mean of –2.95‰, whereas the $\delta^{13}C$ values are from –4.97‰ to –0.42‰ with a mean of –2.45‰. For comparison, analogous data from the nearby Přemyslovice boreholes (see location in Fig. 1) are somewhat different: the $\delta^{18}O$ values range from –1.60‰ to 0.41‰ with a mean of –0.53‰ and the $\delta^{13}C$ values are from –2.72‰ to 0.64‰ with a mean of –0.83‰.

INTERPRETATION AND DISCUSSION

The sedimentary succession

The non-carbonate lower part of the succession (FA1 in Fig. 2) is interpreted as nearshore marine deposits (see facies in Table 1) representing coastal transgression over weathered

List of Bryozoa species and number frequency of taxa found at particular depths in the borehole

Hl-1																				
Bryozoa: Taxa/succession level (cm)	80	130	170	200	230	250	350	410	490	520	580	620	650	690	700	730	780	820	880
Adeonella polystomella (Reuss, 1848)										1									
Biflustra savartii (Savigni et Audouin, 1826)						1									1				
Calpensia gracilis (Münster, 1826)				1															
Cellaria cf. *fistulosa* (Linnaeus, 1758)	1				1		1												
Cellepora indet.	1		1	1	1	1	1	1	1	1	1		1	1	1	1	1	1	1
Cribellopora latigastra (David, 1949)					1														
Crisia hoernesii Reuss, 1848	1																		
Crisidmonea foraminosa (Reuss, 1851)	1			1	1	1													
Disporella goldfussi (Reuss, 1864)																			
Disporella cf. hispida (Fleming, 1828)					1														
Eokotosokum? *bobiesi* (David & Pouyet, 1974)					1														
Escharella tenera (Reuss, 1874)								1											
Exidmonea partschi (Reuss, 1848)																			
Flustrellaria fenestrata (Reuss, 1848)					1														
Heteropora sp.					1	1	1	1	1	1	1			1	1	1		1	1
Hornera cf. *frondiculata* Lamourox, 1821				1															
Margaretta cereoides (Ellis & Solander, 1786)																			
Mecynoecia pulchella (Reuss, 1848)																			
Micropora parvicella Canu & Lecointre, 1927																			
Oncousoecia? *biloba* (Reuss, 1848)				1															
Onychocella angulosa (Reuss, 1848)					1	1													
Ferganula sp.				1	1														
Puellina venusta (Canu & Bassler, 1925)						1													
Umbonula macrocheila (Reuss, 1848)					1														
Ybselosoecia typica (Manzoni, 1878)					1														
Plagioecia rotula (Reuss, 1848)																			
Pleuronea pertusa (Reuss, 1848)																			
Polyascosoecia cancellata Canu, 1920				1															
Reteporella sp.	1		1	1	1	1	1	1		1	1		1	1	1				1
Rhynchozoon monoceros (Reuss, 1848)					1														
Schizomavella protuberans (Reuss, 1847)				1	1														
Smittina cervicornis (Pallas, 1766)				1	1				1										
Tervia irregularis (Meneghini, 1844)					1														
Number of taxa	5	0	2	10	17	7	4	4	3	4	3	0	2	3	4	2	1	2	3

pre-Cenozoic bedrock. The basal surface of these deposits, unreached by the wells but recognizable in georadar sections, is considered to be a ravinement surface of marine flooding. Sediment composition indicates local derivation, apparently by erosional reworking of the terrestrial weathering cover and possibly some fluvial deposits. FA1 shows retrogradational to aggradational style of sediment accumulation, with minor fluctuations in relative sea level probably due to changes in the rate of sediment supply. The main changes in relative sea level, recognizable as fining- upwards cyclothems (Fig. 2), are considered to be parasequences reflecting episodic increases in accommodation, rather than changes in sediment supply. They would then be similar to the "collapsed back-stepping parasequences" of Cattaneo and Steel (2003).

The calcareous upper part of the succession (FA2 in Fig. 2) represents a dramatic decrease in terrigenous sediment input. The boundary between FA1 and FA2 marks an anomalous drop in the concentration of K and Th and the Th/U ratio, and a rise in the Th/K ratio, although the main increase in U relative to other radioactive elements is observed just about 1 m above this boundary. The carbonate facies of FA2 (Table 1) still represent a wave-worked, shallow-marine littoral environment, but the shoreline must have rapidly shifted further landwards, away from the basin, which drastically reduced the delivery of terrigenous sediment.

The retrogradational to incrementally aggradational style of the FA1 deposition thus changed abruptly to a strongly retrogradational style in the lower part of FA2, with the rate of shoreline shift and accommodation growth exceeding the rate of terrigenous sediment supply. As a result, carbonate sedimentation predominated in the study area. The deposits of FA2 are thought to represent a transgressive to highstand systems tract, with the stratigraphic level of highest U concentration probably marking the maximum flooding surface and "absolute minimum" of terrigenous sediment input (see Lüning *et al*., 2003; Doveton and Merriam, 2004; Halgedahl *et al*., 2009).

Table 3

core profiles Hl-1 and Hl-2 (see logs in Fig. 2A, B)

									Hl-2																
900	920	940	980	1000	1040	1080	1100	1150	30	120	180	440	680	890	1080	1130	1240	1350	1410	1550	1620	1680	1720	1820	1950
1	1	1	1	1	1	1	1			1	1	1	1		1	1	1	1	1						
										1		1													
											1														
										1															
											1														
	1	1	1	1	1	1		1		1	1				1	1		1	1						
												1													
	1										1														
										1	1														
1	1																								
										1	1														
												1													
											1														
											1														
											1														
										1	1	1													
	1		1			1		1		1	1					1									
												1													
										1	1														
2	5	2	3	2	2	3	1	2	0	10	13	6	1	0	2	3	1	2	2	0	0	0	0	0	0

The stratigraphic occurrence of carbonates and their relationship with relative sea-level changes in the early Badenian Carpathian Foredeep have long been disputed. The occurrence of limestones within a dominantly siliciclastic succession was attributed variously to marine transgression (Buday, 1955; Hladíková *et al.,* 1992) or regression (Cicha and Dornič, 1960; Krystek and Tejkal, 1968). The present study supports the view of Doláková *et al.* (2008) that the carbonates at the western rim of the basin are related to a transgressive systems tract. The response of carbonate systems to transgression varies, depending upon their morphology and position in the basin (Hladil *et al*., 2006; Kalvoda *et al.*, 2011). In the early Badenian Carpathian Foredeep, it was apparently the temporal decrease in terrigenous sediment input that triggered carbonate sedimentation.

The negative correlation between both K and Th and the clay mineral content in FA1 and FA2 indicates that the main source of these radioactive elements are heavy minerals and detrital mica/feldspar present in the sand and silt fraction, whereas the clay fraction is probably rich in K-poor smectite (see Bersad and Dypvik, 1982).

The heavy-mineral composition indicates garnet derivation from the local suite of metamorphic rocks (metapelites, gneisses, amphibolites and granulites). The provenance of heavy minerals from metapelitic rocks is slightly higher (46.8%) than from the higher-grade metamaphic rocks (42.3%). Most of the rutile grains (88.5%) derive from metamorphic rocks and only the rest from pegmatites. The assemblages of heavy minerals are generally comparable to those in the Culmian sedimentary rocks (Štelcl and Svoboda 1962; Otava, 1998). The predominance of pyrop-almandines was recognized in the Culmian Myslejovice Formation (Čopjaková, 2007). The results of Zr-in-rutile thermometry indicate that 66.6% of the metapelitic rutiles derive from granulite metamorphic facies and 33.3% from amphibolite/eclogite facies.

Table 4

List of Brachiopoda species found at particular depths in the borehole core profile Hl-1 (see log in Fig. 2A)

Hl-1													
Brachiopod taxa/sections	80	200	230	250	350	580	650	690	700	980	1080	1100	1150
Argyrotheca bitnerae Dulai, 2011	1	1	1	1	1				1	1	1	1	
Joania cordata (Risso, 1826)			1			1	1	1	1				1
Platidia sp.			1	1									
Number of species	1	1	3	2	1	1	1	1	2	1	1	1	1

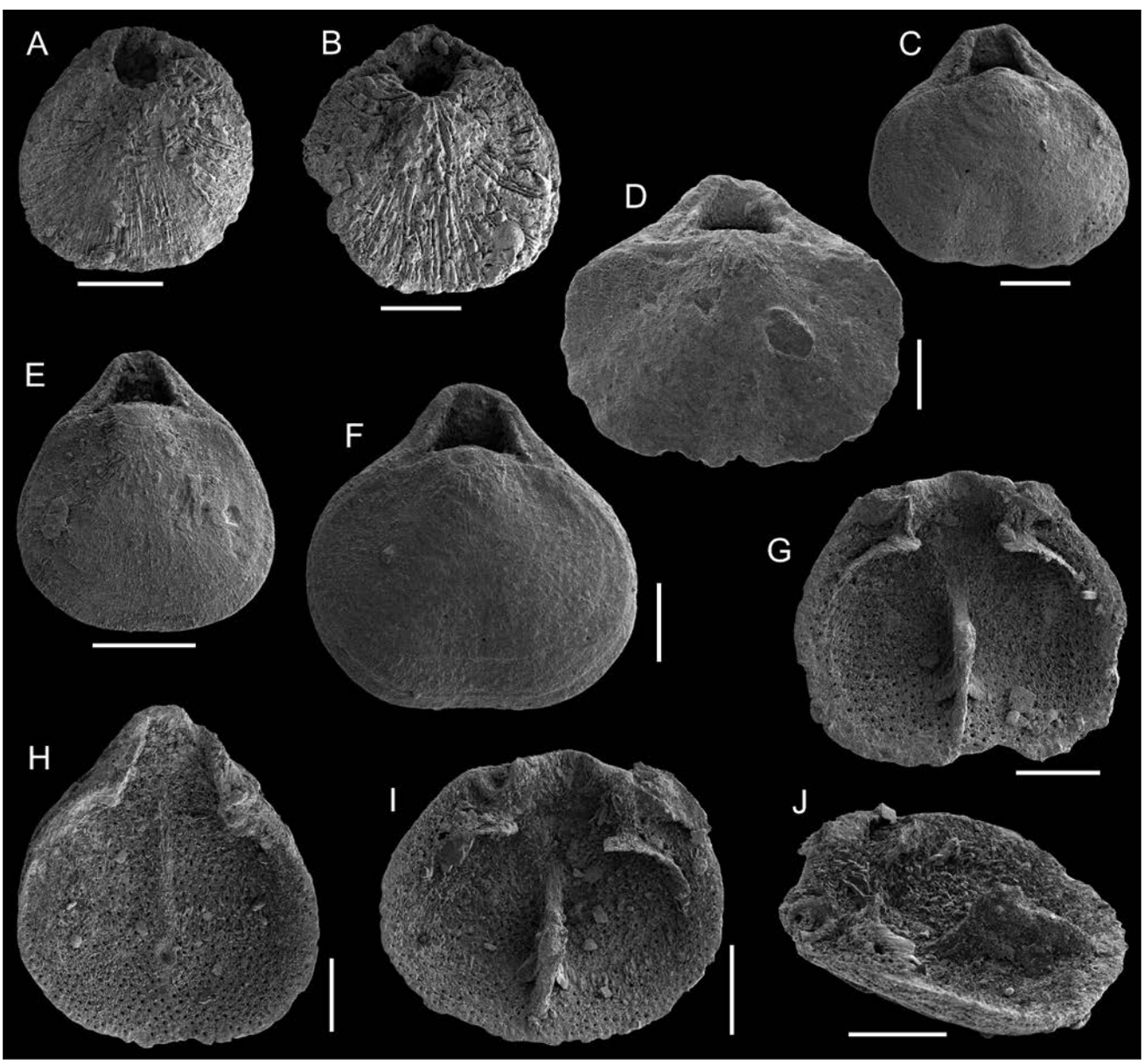

Fig. 4. Examples of Brachiopoda from the Hluchov borehole Hl-1 (SEM images with 0.5 mm scale bars). **A, B.** *Platidia* sp., dorsal views of complete specimens; depth 2.30 m. **C, D.** *Joania cordata* (Risso, 1826), dorsal views of complete specimens; depth 2.30 m and 5.80 m, respectively. **E–J.** *Argyrotheca bitnerae* Dulai, 2011; E – dorsal view of complete specimen, depth 2.00 m; F – dorsal view of complete specimen, depth 11.00 m; G – inner view of dorsal valve, depth 9.80 m; H – inner view of ventral valve, depth 2.30 m; I, J – inner and lateral views of dorsal valve with visible high median septum, depth 2.30 m.

Table 5

List of Mollusca species found at particular depths in the borehole core profiles Hl-1 and Hl-2 (see logs in Fig. 2A, B)

Hl-1																													
Mollusca: taxa/succession level (cm)	80	130	170	200	230	250	350	410	490	520	580	620	650	690	700	730	780	820	880	900	920	940	980	1000	1040	1080	1100	1150
Bivalvia																													
Aequipecten cf. *macrotis* (Sowerby)		1	1		1	1			1		1	1		1					1			1		1	1	1	1	1
Aequipecten cf. *malvinae* (Dubois)			1	1		1			1	1																		1
Aequipecten cf. *scabrellus* (Lamarck)					1	1																						
Aequipecten sp.	1																											
?Anomia sp.		1																1		1				1			1	1
Bivalvia indet.	1	1	1	1					1	1	1	1	1	1	1		1	1	1	1	1	1	1	1			1	
Crassadoma multistriata (Poli)	1	1	1	1	1	1	1		1	1	1	1	1	1	1	1			1		1		1		1	1	1	1
Flexopecten cf. *scissus* (Favre)			1											1												1	1	1
?Glans sp.	1							1	1					1														
"Chlamys" trilirata (Almera & Bofill)			1								1	1		1	1	1	1		1		1	1	1	1	1	1	1	1
Macrochlamis sp.																1							1					
Ostrea cf. *digitalina* (Dubois)											juv			juv	1		juv	juv	1	1	1	1	juv		juv	juv		
Ostrea sp.															juv.					1								1
Ostreidae indet.	1	1		1		1		1	1	1	1	1	1	1	1	1	1	1	1	1	1	1	1	1	1	1	1	
Pecten subarcuatus styriacus Hilber		1											1		1													
Pectinidae indet.	1	1	1	1	1	1	1	1	1	1	1	1	1	1	1	1	1	1	1	1	1	1	1	1	1	1	1	1
Spondylus sp.											1		1															
Gastropoda																												
?Petaloconchus intortus (Lamarck)																	1	1										
Scaphopoda																												
Scaphopoda indet.		1				1	1		1																			

juv – juvenile

Hl-2																		
Mollusca: taxa/sections (cm)	30	120	180	440	680	890	1080	1130	1240	1400	1400	1600	1600	1700	1700	1800	1950	
Bivalvia																		
Aequipecten cf. macrotis (Sowerby)					1										1	1		
Aequipecten cf. malvinae (Dubois)													1					
Aequipecten cf. *scabrellus* (Lamarck)												1						
Aequipecten sp.			1			1												
Bivalvia indet.	1	1	1			1		1	1	1	1	1	1	1	1	1	1	
Crassadoma multistriata (Poli)		1		1		1			1	1			1	1	1	1	1	
Flexopecten scissus (Favre)													1	1	1	1	1	
?*Glans* sp.								1										
"Chlamys" trilirata (Almera & Bofill)										1	1		1					

The stratigraphic variation in heavy-mineral assemblages indicates changes in the sediment provenance, probably related to the landward extent and variable morphology of the transgressive shoreline. The deposits of FA1 consist of sediment derived from the local substrate, whereas the terrigenous component in the deposits of FA2 suggests sediment derivation from a broader source area, with an input of freshly weathered material and volcanic tephra. This change in sediment provenance is reflected in the plot of Th/K against Th/U (Fig. 2B). The volcanogenic component is comparable to the early Badenian tephra known from the Carpathian Foredeep as a product of paroxysmal rhyolitic to rhyodacitic eruptions (Nehyba *et al*., 1999). The stratigraphic level enriched in volcanogenic minerals can be correlated with the thick beds of airfall tephra found *ca.* 6 km to the NW near Přemyslovice (Zágoršek *et al*., 2012).

The early Badenian marine transgression is attributed to a eustatic sea-level rise of the global cycle TB 2.4 (Haq *et al.,*

Table 6

List of other fossil groups found at particular depths in the borehole core profiles Hl-1 and Hl-2 (see logs in Fig. 2A, B)

Hl-1																												
Other fossils: succession level (cm)	80	130	170	200	230	250	350	410	490	520	580	620	650	690	700	730	780	820	880	900	920	940	980	1000	1040	1080	1100	1150
Echinodemata	2	2	1	2	2	2	2	2	2	2	1	1	1	1	1	1	1	1	1	1	1	1	1	1	1	1	1	1
Cirripedia	2	1	1	1	2	2	2	2	2	2	1	2	2	1	1	1	1	1	1	1	1	1	1	1	1	1	1	1
Vermes		1	1				1	1	1	ot	1		1	1	1	1	1	1	1	1	1	1		1	1	1	1	1
Teleostei	1		1		1	1			1	1	1	1			1									1				
Anthozoa																									1			

Hl-2																	
Other fossils: succession level (cm)	30	120	180	440	680	890	1080	1130	1240	1350	1410	1550	1620	1680	1720	1820	1950
Echinodermata			1	1	1	1	1	1	1	1	1		1	1	1	1	1
Cirripedia				1	1	1	2	2	1	1	1	1	1	1	1		1
Vermes		1	1														
Teleostei	ot																
Corallinaceae	1		1	1	1					1				1	1		1

ot – otoliths

1988, Hohenegger *et al*., 2014). The abruptness of the transgression, with littoral deposits covering directly subaerial weathered substrate, and the transgression wide regional extent on the crystalline Bohemian Massif (Hladilová *et al*., 1999; Zagoršek *et al.,* 2009) can be attributed to the low topographic relief of forebulge flank. It is possible that the eustatic sea-level rise coincided with a phase of the forebulge subsidence and retreat, which would enhance further the rate and areal extent of transgression (see discussion in Leszczyński and Nemec, 2014). The notion of a tectonically-forced growth of forebulge accommodation is supported by the evidence of fining-upwards parasequences in FA1 and the ultimate stratigraphic change of FA1 into FA2 (Fig. 2), which both have no obvious eustatic explanation.

Biostratigraphy

Planktonic species are crucial for stratigraphic interpretations based on foraminifers. However, the foraminifer assemblages from borehole Hl-1 consist mainly of benthic taxa and hence are difficult to assign to specific biozones. The composition of these assemblages and their stratigraphic and lithofacies context allow the age of deposits to be estimated only as the early Badenian. *Pappina breviformis* was earlier considered as indicative of Karpatian (*sensu* Papp and Turnovsky, 1958), but newer studies (Cicha *et al.*, 1998; Rögl and Spezzaferri, 2003) have shown that it may also indicate the early Badenian.

Supportive biostratigraphic evidence comes from pectinid species. *Costellamussiopecten spinulosus* is a characteristic Badenian taxon, typical only for the upper part of the lower Badenian (the Upper Lagenidae Zone of Mandic, 2004; the Mid-Badenian *sensu* Hohenegger *et al.*, 2014). The first occurrences (FOs) of *Aequipecten malvinae* (a continuous Badenian species) and "*Chlamys*" *trilirata* (occurring only in the lower to ?middle Badenian) in the Paratethys realm are positioned above the base of the middle Miocene (Mandic, 2004). The mollusc fauna thus supports the early Badenian age of deposits inferred from foraminifers.

Some of the pectinid species in the Hluchov borehole Hl-1 have been reported from the Grund Formation in the Alpine–Carpathian Foredeep of Lower Austria, correlated with the Lower Lagenidae Zone (Mandic, 2004). The absence of *Costellamussiopecten spinulosus* in the Grund Formation indicates that its deposits are slightly older than the deposits in the Hluchov area and also those reported from the Kralice nad Oslavou and Židlochovice areas (Zágoršek *et al*., 2009; Doláková *et al.*, 2014).

Palaeoecology

The foraminifer assemblages from the borehole core Hl-1 indicate a marine palaeoenvironment with unstable salinity, perhaps brackish or hypersaline. Towards the top of the succession, ammonias are replaced by elphidia, which inhabit warm and shallow (2 m) sea waters. Taphonomic analysis indicates that the shells of more cryophilic (deeper-water) species are usually more damaged and corroded, whereas shells of typical shallow-water species usually (though not always) have preserved their sculptures. At the core depth of 7.80 m (Fig. 2A), the foraminifers are absent, although there is a surprising occurrence of other fauna. It is unclear as to whether we are dealing here with a mixed fauna association, as in the adjacent Přemyslovice borehole cores (where, however, two types of association were recognized; Zágoršek *et al*., 2012), or whether the species are *in situ* at the lower boundary of their occurrence.

Bryozoans are generally indicative of a fully marine (salinity ~35‰), warm-water environment dominated by suspension-feeder fauna. The abundant bryozoan association of *Reteporella* and new species of *Cribellopora* indicates a high water-energy environment.

The brachiopods are exclusively marine, sessile invertebrates that can occur at a wide range of water depth and

Table 7

The carbon and oxygen stable isotope composition of early Badenian mollusc shells at particular depths in the borehole core profiles Hl-1 and Hl-2 (see logs in Fig. 2A, B)

Sample/succession level	^{13}C	^{18}O	Species
Hl-1			
Hl-1/1 (130 cm)	–0.94	–3.43	*Crassadoma multistriata*
Hl-1/2 (200 cm)	–2.11	–3.45	*Crassadoma multistriata*
Hl-1/3 (520 cm)	–-4.88	–4.14	*Crassadoma multistriata*
Hl-1/4 (580 cm)	–4.38	–4.36	*Crassadoma multistriata*
Hl-1/5A (690 cm)	–3.46	–2.46	*Crassadoma multistriata*
Hl-1/6 (700 cm)	–2.41	–4.61	*Crassadoma multistriata*
Hl-1/7 (880 cm)	–0.42	–3.98	*Crassadoma multistriata*
Hl-1/8 (920 cm)	–2.00	–1.62	*Crassadoma multistriata*
Hl-1/9 (1040 cm)	–1.99	–2.35	*Crassadoma multistriata*
Hl-1/10A (1080 cm)	–3.56	–3.54	*Crassadoma multistriata*
Hl-1/11 (1150 cm)	–1.43	–2.92	*Crassadoma multistriata*
Hl-1/12 (130 cm)	–1.51	–2.82	*Aequipecten macrotis*
Hl-1/13 (200 cm)	–4.97	–3.33	*Flexopecten scissus*
Hl-1/14 (520 cm)	–4.49	–2.43	Pectinidae indet.
Hl-1/15 (580 cm)	–4.06	–4.21	Pectinidae indet.
Hl-1/16 (690 cm)	–3.03	–1.69	*Flexopecten scissus*
Hl-1/17 (700 cm)	–2.07	–3.47	*Chlamys trilirata*
Hl-1/18 (880 cm)	–1.80	–2.69	*Chlamys trilirata*
Hl-1/19 (920 cm)	–1.93	–2.04	*Chlamys trilirata*
Hl-1/20 (1040 cm)	–1.88	–2.60	*Chlamys trilirata*
Hl-1/21 (1080 cm)	–2.67	–2.08	*Flexopecten scissus*
Hl-1/22 (1150 cm)	–2.66	–3.04	*Flexopecten scissus*
Hl-2			
Hl-2/1 (120 cm)	–1.26	–2.18	*Crassadoma multistriata*
Hl-2/2 (440 cm)	–3.49	–3.99	*Crassadoma multistriata*
Hl-2/3 (1240 cm)	–0.89	–3.10	*Crassadoma multistriata*
Hl-2/4 (1620 cm)	–0.83	–1.60	*Crassadoma multistriata*
Hl-2/5 (1820 cm)	–1.14	–2.37	*Crassadoma multistriata*
Hl-2/6 (1950 cm)	–0.52	–2.35	*Crassadoma multistriata*
Hl-2/7 (120 cm)	–4.02	–3.75	Bivalvia indet.
Hl-2/8 (440 cm)	–5.65	–4.68	Pectinidae indet.
Hl-2/9 (1240 cm)	–2.69	–3.79	Pectinidae indet.
Hl-2/10 (1620 cm)	–2.65	–3.35	*Flexopecten scissus*
Hl-2/11 (1820 cm)	–1.69	–2.04	*Flexopecten scissus*
Hl-2/12 (1950 cm)	–1.74	–1.97	*Flexopecten scissus*

hence are bathymetrically non-diagnostic. For example, the recent representatives of megathyrids (*Argyrotheca*, *Joania*) and *Platidia* can live at water depths ranging from a few metres to more than 1000 m (Logan, 2007). Middle Miocene brachiopods have been reported from many sites of the Central Paratethys (e.g., Bitner, 1990; Bitner and Kaim, 2004; Dulai and Stachacz, 2011), but are still little-known from the Carpathian Foredeep (see Zágoršek *et al.*, 2012, Bitner *et al*., 2013, Pavézková *et al.,* 2013).

The molluscan fauna is predominantly stenohaline (Pectinidae dominate among bivalves), with brackish or estuarine species absent, which supports the notion of a fully marine (salinity ~35‰) palaeoenvironment. This evidence is consistent with that from brachiopods and bryozoans and with the abundant occurrence of echinoderms in both borehole cores.

Table 8

Comparative dataset on the carbon and oxygen stable isotope composition of early Badenian mollusc shells at particular depths in the nearby Přemyslovice borehole cores PY-5–7 (see location in Fig. 1)

Sample/succession level	^{13}C	^{18}O	Species
PY-5			
PY-5/1 (40 cm)	–1.69	–1.60	*Crassadoma multistriata*
PY-5/2 (100 cm)	0.19	–0.03	*Crassadoma multistriata*
PY-5/3 (40 cm)	0.64	–0.38	*Aequipecten macrotis*
PY-5/4 (100 cm)	–2.66	–0.65	*Flexopecten scissus*
PY-6			
PY-6/1 (30 cm)	0.42	–0.57	*Crassadoma multistriata*
PY-6/2 (60 cm)	0.01	–1.07	*Crassadoma multistriata*
PY-6/3 (150 cm)	0.59	–0.13	*Crassadoma multistriata*
PY-6/4 (165 cm)	0.34	–0.47	*Crassadoma multistriata*
PY-6/5 (30 cm)	–1.74	–0.97	*Flexopecten scissus*
PY-6/6 (60 cm)	–2.53	0.41	*Flexopecten scissus*
PY-6/7 (150 cm)	0.06	–0.28	*Flexopecten scissus*
PY-6/8 (165 cm)	–2.72	–1.13	*Flexopecten scissus*
PY-7			
PY-7/1 (150 cm)	–0.28	–0.66	*Crassadoma multistriata*
PY-7/2 (180 cm)	–0.90	–1.13	*Crassadoma multistriata*
PY-7/3 (150 cm)	–2.15	0.71	*Flexopecten scissus*

as a function of borehole depth (Fig. 6) shows a significant

The lower parts of the borehole profiles show a high amount of molluscan shell fragments, mainly oysters (*Ostrea digitalina*), even juvenile, and pectinids. The admixture of species from exposed rocky intertidal and shallow subtidal habitats indicates a high-energy seawater conditions. Epibionts dominanate, derived from hard-substrate habitats. The molluscan shells commonly show evidence of drilling, bioerosion, corrosion and dissolution, indicating a fluctuating and often low rate of sediment accumulation.

The upper parts of both borehole profiles are dominated by pectinids. Oysters are rare, some species (like *Ostrea digitalina*) are even absent, and shell fragments are relatively few. The dominance of infralittoral (shallow subtidal) taxa indicates deeper and lower-energy seawater conditions, with the sea floor inhabited mainly by suspension feeders. This evidence supports the notion of FA2 representing a marine transgression.

Isotopic evidence

Stable carbon and oxygen isotope compositions show a generally positive correlation (Fig. 5) between the mollusc shells from the Hluchov boreholes and samples enriched in heavy isotopes from the nearby Přemyslovice boreholes (Fig. 1). The upper limit of the $\delta^{13}C$ and $\delta^{18}O$ values is close to the normal marine compositions, while most of the studied samples have values shifted in negative direction by several per mille (‰). The extent of these isotope shifts indicates that diagenesis may have played an important role in determining the isotope compositions. A plot of the isotope compositions

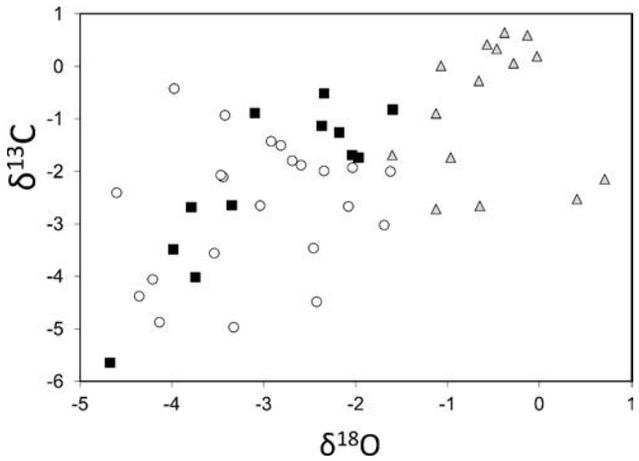

Fig. 5. Carbon and oxygen stable isotope compositions (values in ‰ relative to V-PDB) of molluscan shells from the Hluchov boreholes (Hl-1: open circles; Hl-2: solid squares) and for comparison from the Přemyslovice boreholes (PY-5, 6, 7: grey triangles).

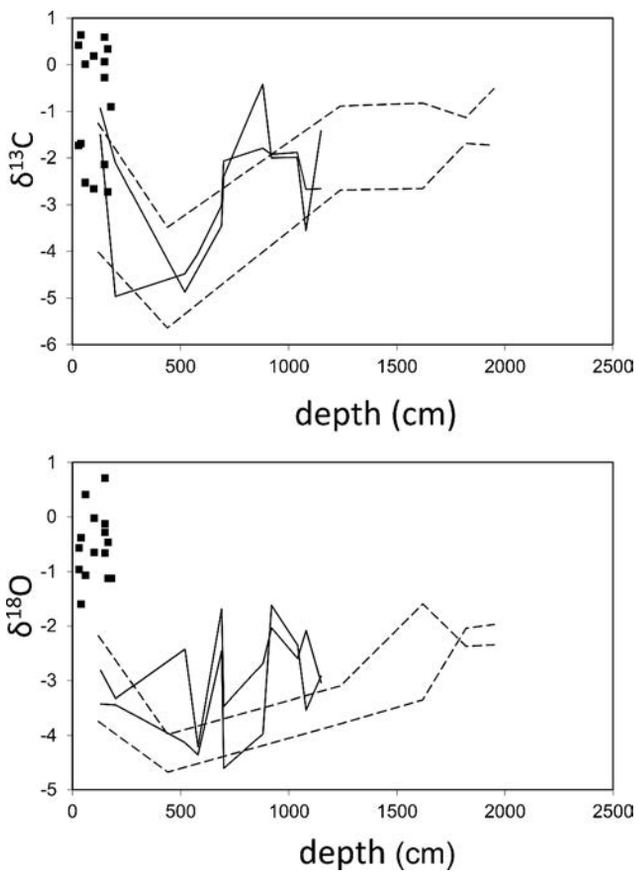

Fig. 6. Plots showing variation in the carbon and oxygen stable isotope compositions of molluscan shells (values in ‰ relative to V-PDB) with borehole depth. Data from the Hluchov boreholes (Hl-1: solid lines; Hl-2: dashed lines) and Přemyslovice boreholes (PY-5, 6, 7: solid squares).

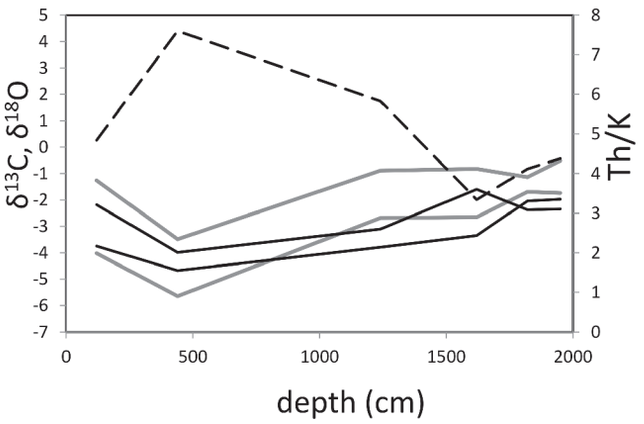

Fig. 7. Comparative plot of the variation in carbon (grey solid line) and oxygen (black solid line) stable isotope compositions of molluscan shells and the hostrock bulk Th/K ratio (dashed line) with borehole depth. Data from borehole Hl-2; isotopic values in ‰ relative to V-PDB; the Th/K ratio derived from gamma-ray spectrum.

isotopic difference between the Přemyslovice and Hluchov localities. On the basis of carbon isotope compositions, samples from the upper part of the Hluchov profile could be correlated with the Přemyslovice samples, but the oxygen isotope compositions at the former locality are much lower than in the latter. The strong negative shifts of $\delta^{18}O$ in the Hluchov samples may be due to diagenetic alteration.

The shells from Hluchov boreholes show marked interspecies differences, with the *Crassadoma* shells generally richer in ^{13}C and ^{18}O than the *Flexopecten, Aequipecten* and *Chlamys* shells (Fig. 6). This difference is most remarkable in the profile of borehole Hl-2, but less pronounced or even obscured in the profile of borehole Hl-1, probably due to the homogenizing effect of diagenetic alteration.

The fluctuations of isotope composition with borehole depth seem to be related to lithofacies changes. More permeable layers may serve as conduits for diagenetic fluids, and the corresponding isotope shifts in these layers will then be more pronounced. Siliciclastic layers within a carbonate succession may be such diagenesis-sensitive levels. However, the concentrations of K and Th are lower in that part of the Hl-2 profile where shells show strongly negative isotopic shifts. The plot of Th/K and isotope composition data (Fig. 7) may be a clue to understand the influence of diagenetic processes. Elevated Th/K ratios are found in the layers with strongly negative $\delta^{13}C$ and $\delta^{18}O$ values, and thus affected by diagenetic alteration. The enrichment in Th relative to K suggests that the sediment permeability was determined by the content of clay minerals, rather than siliciclastic detritus. A lower amount of clays (higher Th/K ratio) would mean greater permeability and stronger effects of diagenetic fluids.

CONCLUSIONS

Deposits recording an early Badenian marine transgression were found in boreholes Hl-1 and Hl-2 near Hluchov, on the outer flank of the Western Carpathian Foredeep in the Czech Republic. The basal nearshore marine deposits reflect coastal transgression over a terrestrial topography of weathered pre-Cenozoic bedrock. The lower facies association (FA1) is chiefly siliciclastic, with sediment of local provenance derived by substrate erosion. Sedimentary facies indicate a wave-dominated environment with unstable sandy bottom, variable rate of sediment supply and an incremental rise of relative sea level. The upper facies association (FA2) consists of shallow-marine carbonates indicating a major landward shift of the shoreline, a dramatic decrease in siliciclastic sediment input and a continuing rise of relative sea level. The whole succession was deposited as a shallow-marine transgressive to highstand systems tract.

The boundary between the FA1 and FA2 parts of the successions is marked by an anomalous decrease in the concentration of K and Th and the Th/U ratio, a rise in the Th/K ratio and the highest U concentration, which are considered to signify the maximum marine flooding surface – recognized about 1 m above the FA1/FA2 boundary. The study supports the view of Doláková *et al.* (2008) that the Badenian carbonates and particularly red-algal limestones along the outer fringe of the Western Carpathian Foredeep are a result of major marine transgression, which shifted the shoreline landwards with relatively little deepening of the forebulge littoral environment.

The heavy-mineral assemblages in FA1 confirm local sediment derivation, whereas those in FA2 indicate a broader sediment provenance, including airfall tephra from contemporaneous rhyolitic to rhyodacitic volcanism documented elsewhere in the foredeep basin (Nehyba *et al.,* 1999; Zágoršek *et al*., 2012).

The deposits in the Hluchov borehole cores abound in fossils, such as Foraminifera (mainly benthic), Bryozoa, Brachiopoda, Mollusca (Bivalvia, Scaphopoda), Echinodermata (Echinoidea, Asteroidea, Ophiuroidea), Arthropoda (Cirripedia), Vermes, occasional Teleostei and rare Anthozoa. Only the foraminifers and molluscs are biostratigraphically diagnostic, indicating an early Badenian age of the deposits. The molluscs, bryozoans and echinoderms confirm a normal-salinity marine environment with a gradually decreasing hydraulic energy, and the foraminifers indicate some salinity fluctuations in the lowest part of the Hl-1 borehole profile. The palaeontological evidence is consistent with the sedimentological facies evidence of a stepwise marine transgression.

The isotopic composition of mollusc shells from the Hluchov boreholes shows marked inter-species differences, with the *Crassadoma* shells generally richer in ^{13}C and ^{18}O relative to the *Flexopecten, Aequipecten* and *Chlamys* shells. Most of the mollusc shells show a negative shift by several ‰ in their $\delta^{13}C$ and $\delta^{18}O$ values, which indicates an impact of diagenetic processes. There is also a significant difference in the isotopic composition of mollusc shells between the Hluchov and nearby Přemyslovice borehole cores, attributed to the lateral variation in sedimentary facies and their differential sensitivity to diagenetic changes.

Elevated Th/K ratios are found in the layers with highly negative $\delta^{13}C$ and $\delta^{18}O$ values, which means most affected by diagenetic alteration. The high amount of Th relative to K indicates low clay content, suggesting that sediment permeability played crucial role in the circulation and differential effect of diagenetic fluids.

The study as a whole contributes to a better understanding of the Neogene palaeogeographic development in the Western Carpathian Foredeep, while demonstrating also the range of sedimentological, palaeontological and geochemical signatures that characterize major marine transgression on the low-relief peripheral bulge of a foredeep basin.

Acknowledgements

The study was sponsored by project grant 205/09/0103 from the Grant Agency of the Czech Republic and by Research Project 321360 (Czech Geological Survey). Šárka Roušavá (Masaryk University) kindly improved the written English of an earlier version of the manuscript. We thank Stanisław Leszczyński (Jagiellonian University) and Michael Wagreich (Vienna University) for helpful critical reviews, and Wojciech Nemec (Bergen University) for editing and improving the manuscript.

REFERENCES

Berstad, S. & Dypvik, H., 1982. Sedimentological evolution and natural radioactivity of Tertiary sediments from the central North Sea. *Journal of Petroleum Geology*, 5: 77–88.

Bitner, M. A., 1990. Middle Miocene (Badenian) brachiopods from the Roztocze Hills, south-eastern Poland. *Acta Geologica Polonica*, 40: 129–157.

Bitner, M. A. & Kaim, A., 2004. The Miocene brachiopods from the silty facies of the intra-Carpathian Nowy Sącz Basin (Poland). *Geological Quarterly*, 48: 193–198.

Bitner, M. A., Zágoršek, K. & Hladilová, Š., 2013. Deep-water brachiopod assemblage from the Middle Miocene of Kralice nad Oslavou, Moravia, southeastern Czech Republic. *Comptes Rendus Palevol*, 12: 81–89.

Bubík, M. & Dvořák, J., 1996. O nálezu karpatu (miocén) a dalších výsledcích vrtu Slatinky MH-10. *Zprávy o geologických výzkumech v roce 1995*, pp. 20–21. [In Czech.]

Buday, T., 1955. Současný stav stratigrafického výzkumu ve spodním a středním miocénu na dolní Moravě. *Věstník Ústředního ústavu geologického*, 30: 162–168. [In Czech.]

Burbank, D. W. & Beck, R. A., 1991. Models of aggradation versus progradation in the Himalayan Foreland. *Geologische Rundschau*, 80: 623–638.

Cattaneo, A. & Steel, R. J., 2003. Transgressive deposits: a review of their variability. *Earth-Science Reviews*, 62: 187–228.

Cicha, I. & Dornič, J., 1960. Miocenní vývoj boskovické brázdy mezi Tišnovem a Ústí nad Orlicí. *Sborník Ústředního ústavu geologického*, *Geologia*, 26: 393–434. [In Czech.]

Cicha, I., Rögl, F., Rupp, Ch. & Čtyroká, J., 1998. Oligocene–Miocene foraminifera of the Central Paratethys. *Abhandlungen der Senckenbergischen Naturforschenden Gesellschaft*, 549: 1–325.

Čopjaková, R., 2007. *Odraz změn provenience v psefitické a psamitické frakci sedimentů myslejovického souvrství (analýza těžkých minerálů)*. Unpublished Ph.D. Thesis, Masaryk University, Brno. [In Czech.]

Doláková, N., Brzobohatý, R., Hladilová, Š. & Nehyba, S., 2008. The red algal facies of the Lower Badenian limestones of the Carpathian Foredeep in Moravia (Czech Republic). *Geologica Carpathica,* 59: 133–146.

Doláková, N., Holcová, K., Nehyba, S., Hladilová, Š., Brzobohatý, R., Zágoršek, K., Hrabovský, J., Seko, M. & Utescher, T., 2014. The Badenian parastratotype at Židlochovice from the perspective of the multiproxy study. *Neues Jahrbuch für Geologie und Paläontologie, Abhandlungen,* 271: 169–201.

Doveton, J. H. & Merriam, D. F., 2004. Borehole petrophysical chemostratigraphy of Pennsylvanian black shales in the Kansas subsurface. *Chemical Geology*, 206: 249–258.

Dulai, A. & Stachacz, M., 2011. New Middle Miocene *Argyrotheca* (Brachiopoda; Megathyrididae) species from the Central Paratethys. *Földtani Közlöny*, 141: 283–291.

Flemings, P. B. & Jordan, T. E., 1989. Stratigraphic modelling of foreland basins: Interpreting thrust deformation and lithospere rheology. *Geology*, 18: 430–434.

Folk, R. L. & Ward, W., 1957. Brazos River bar: a study in the significance of grain-size parameters. *Journal of Sedimentary Petrology*, 27: 3–26.

Force, E. R., 1980. The provenance of rutile. *Journal of Sedimentary Petrology*, 50: 485–488.

Haq, B. U., Hardenbol, J. & Vail, P. R., 1988. Mesozoic and Cenozoic chronostratigraphy and eustatic cycles. In: Wilgus, C. K., Hastings, B .S., Posamentier, H., van Wagoner, J., Ross, C. A. & Kendall, C. G. S. C. (eds), *Sea-level Changes: An Integrated Approach*. SEPM Special Publication, 42: 71–108.

Halgedahl, S. L., Jarrard, R. D., Brett, C. E. & Allison, P. A., 2009. Geophysical and geological signatures of relative sea level change in the upper Wheeler Formation, Drum Mountains, West-Central Utah: A perspective into exceptional preservation of fossils. *Palaeogeography Palaeoclimatology Palaeoecology*, 277: 34–56.

Harloff, J. & Mackensen, A., 1997. Recent benthic foraminiferal associations and ecology of the Scotia Sea and Argentine Basin. *Marine Micropalaeontology*, 31: 1–29.

Hilgen, F. J., Lourens, L. J., Van Dam, J. A., Beu, A. G., Boyes, A. F., Cooper, R. A., Krijgsman, W., Ogg, J. G., Piller, W. E. & Wilson, D. S., 2012. The Neogene Period. In: Gradstein, F. M., Ogg, J. G., Schmitz, M. D. & Ogg, G. M. (eds), *The Geologic Time Scale 2012*. Elsevier, Amsterdam, pp. 923–978.

Hladil, J., Geršl, M., Strnad, L., Frána, J., Langrová, A. & Spišiak, J., 2006. Stratigraphic variation of complex impurities in platform limestones and possible significance of atmospheric dust: a study with emphasis on gamma-ray spectrometry and magnetic susceptibility outcrop logging (Eifelian-Frasnian, Moravia, Czech Republic). *International Journal of Earth Sciences*, 95: 703–723.

Hladilová, S., Nehyba, S., Dolákova, N. & Hladíková, J., 1999. Comparison of some relics of Miocene sediments on the eastern margin of the Bohemian Massif. *Geologica Carpathica*, 50 (Special Issue): 31–33.

Hladíková, J., Hladilová, Š. & Nehyba, S., 1992. Preliminary results of new investigations of Miocene sediments of Hostim (SW Moravia). In: Hamršmíd, B. (ed.), *New Results on Tertiary of the Western Carpathians. Knihovnička Zemního Plynu Nafty*, 15: 165–176.

Hohenegger, J., Ćorić, S. & Wagreich, M., 2014. Timing of the Middle Miocene Badenian Stage of the Central Paratethys. *Geologica Carpathica*, 65: 55–66.

Hudáčková, N., 1995. Ecotype variability of genus *Ammonia* Brünnich 1772 in the Neogene of Paratethys and their paleoecological significance. *Mineralia Slovaca*, 27: 133–144.

Ingle, J. C., Jr., 1980. Cenozoic paleobathymetry and depositional history of selected sequences within the Southern California continental borderland. In: Sliter, W. V. (ed.), *Studies in Marine Micropaleontology and Paleoecology: Memorial Volume to Orville L. Bandy. Cushman Foundation for Foraminiferal Research, Special Publication, 19*: 163–195.

Jašková, V., 1998. Nově objevené miocénní lokality na Prostějovsku. *Přírodovědné studie Muzea Prostějovska*, 1: 133–139. [In Czech.]

Johnson, D. C. & Beaumont, C., 1995. Preliminary results from a platform kinematic model of orogen evolution, surface processes and the development of clastic foreland basin stratigraphy. In: Dorobek, S. L. & Ross, G. M. (eds), *Stratigraphic Evolution of Foreland Basins. SEPM Special Publication,* 52: 1–24.

Kalabis, V., 1961. Historie výzkumu terciéru širšího okolí Prostějova. *Sborník Vlastivědného Muzea v Prostějově*, *Oddíl přírodovědný*, pp. 59–75. [In Czech.]

Kalvoda, J., Bábek, O., Devuyst, F. X. & Sevastopulo, G. D., 2011. Biostratigraphy, sequence stratigraphy and gamma-ray spectrometry of the Tournaisian–Viséan boundary interval in the Dublin Basin. *Bulletin of Geosciences*, 86: 683–706.

Krystek, I. & Tejkal, J., 1968. Zur Lithologie und Stratigraphie des Miozäns in sw. Teile der Karpatischen Vortiefe in Mähren. *Folia Facultatis Scientiarum Naturalium Universitatis Purkynianae Brunensis, Geologia*, 9: 1–31. [In German.]

Langmuir, D. & Herman, J. S., 1980. The mobility of thorium in natural waters at low temperatures. *Geochimica et Cosmochimica Acta,* 44: 1753–1766.

Leszczyński, S. & Nemec, W., 2014. Dynamic stratigraphy of composite peripheral unconformity in a foredeep basin. *Sedimentology*, doi: 10.1111/sed.12155.

Logan, A., 2007. Geographic distribution of extant articulated brachiopods. In: Selden, P. A. (ed.), *Treatise on Invertebrate Paleontology, Part H. Brachiopoda Revised. Volume 6.* Geological Society of America and University of Kansas, Boulder (Colorado) and Lawrence (Kansas), pp. 3082–3115.

Lüning, S., Adamson, K. & Craig, J., 2003. Frasnian organic-rich shales in North Africa; regional distribution and depositional model. In: Artur, T., MacGregor-Duncan, S. & Cameron, N. R. (eds), *Petroleum Geology of Africa: New Themes and Developing Technologies. Geological Society of London, Special Publications,* 207: 165–184.

Mandic, O., 2004. Pectinid bivalves from the Grund Formation (Lower Badenian, Middle Miocene, Alpine-Carpathian Foredeep) – taxonomic revision and stratigraphic significance. *Geologica Carpathica*, 55: 129–146.

Matenco, L., Krézsek, C., Merten, S., Schmid, S., Cloetingh, S. & Andriessen, P., 2010. Characteristics of collisional orogens with low topographic build-up: an example from the Carpathians. *Terra Nova*, 22: 155–195.

Meinhold, G., Anders, B., Kostopoulos, D. & Reischmann, T., 2008. Rutile chemistry and thermometry as provenance indicator: An example from Chios Island, Greece. *Sedimentary Geology*, 203: 98–111.

Mísař, Z., Dudek, A., Havlena, V. & Weiss, J., 1983. *Geologie ČSSR, I – Český Masiv*. SNTL, Praha, 333 pp. [In Czech.]

Murray, J., 2006. *Ecology and Applications of Benthic Foraminifera.* Cambridge University Press, Cambridge, 426 pp.

Müller, V., Čurda, J., Manová, M., Otava, J., Pačesová, E., Rejchrt, M., Rýda, K. & Šalanský, K., 2000. Vysvětlivky k souboru geologických a ekologických účelových map přírodních zdrojů v měřítku 1 : 50 000, list 24-21 Jevíčko. In: *Soubor geologických a ekologických účelových map*. Czech Geological Survey, Praha, 62 pp. [In Czech.]

Nehyba, S., Roetzel, R. & Adamová, M., 1999. Tephrostrati- graphy of the Neogene volcaniclastics (Moravia, Lower Austria, Poland). *Geologica Carpathica,* 50 (Special Issue): 126– 128.

Nehyba, S. M & Jašková, V., 2012. Výsledky vrtného průzkumu na lokalitě Hluchov (sedimenty spodního badenu karpatské předhlubně). *Geologické výzkumy na Moravě a ve Slezsku v roce 2011*, 19: 36–41. [In Czech.]

Nehyba, S. & Šikula, J., 2007. Depositional architecture, sequence stratigraphy and geodynamic development of the Carpathian Foredeep (Czech Republic). *Geologica Carpathica*, 58: 53–69.

Nemec, W., 2005. *Principles of Lithostratigraphic Logging and Facies Analysis*. Course GEOV360 Lecture Notes, University of Bergen, 28 pp.

Novák, Z., 1975. *Spodnobadenské vápence karpatské předhlubně*. Unpublished Ph.D. Thesis, Masaryk University, Brno. [In Czech.]

Otava, J., 1998. Trendy změn ve složení siliciklastik drahanského kulmu a jejich geotektonická interpretace. *Geologické výzkumy na Moravě a ve Slezsku v roce 1997,* 5: 62–64. [In Czech.]

Papp, A. & Turnovsky, K., 1953. Die Entwicklung der Uvigerinen im Vindobon (Helvet und Torton) des Wiener Beckens. *Jahrbuch der Geologischen Bundesanstalt*, 96: 117–143. [In German.]

Pavézková, J., Hladilová, Š. & Bitner, M. A., 2013. Miocene brachiopods from the Židlochovice locality, Czech Republic. *Geological Research in Moravia and Silesia*, 20: 56–59.

Powers, M. C., 1982. *Comparison Chart for Estimating Roundness and Sphericity*. AGI Data Sheet 18.

Pupin, J. P., 1980. Zircon and granite petrology. *Contribution to Mineralogy and Petrology*, 73: 207–220.

Reading, H. G. (ed.), 1996. *Sedimentary Environments: Processes, Facies and Stratigraphy.* Blackwell Scientific Publications, Oxford, 593 pp.

Royden, L. H., 1993. Evolution of retreating subduction boundaries formed during continental collision. *Tectonics*, 12: 629– 638.

Royden, L. H. & Burchfiel, B. C., 1989. Are systematic variations in thrust belt style related to plate boundary processes? (the Western Alps versus the Carpathians). *Tectonics*, 8: 51–61.

Rögl, F. & Spezzaferri, S., 2003. Foraminiferal paleoecology and biostratigraphy of the Mühlbach section (Gaindorf Formation, Lower Badenian), Lower Austria. *Annalen des Naturhistorischen Museums in Wien*, 104A: 23–75.

Sinclair, H. D., 1997. Tectonostratigraphic model for underfilled peripheral foreland basin: An Alpine perspective. *Bulletin of the Geological Society of America*, 109: 324–346.

Spötl, C. & Vennemann, T. W., 2003. Continuous-flow isotope ratio mass spectrometric analysis of carbonate minerals. *Rapid Communications in Mass Spectrometry*, 17: 1004–1006.

Stendal, H., Toteu, S. F., Frei, R., Penaye, J., Njel, U. O., Bassahak, J., Nni, J., Kankeu, B., Ngako, V. & van Hell, J., 2006. Derivation of detrial rutile in the Yaoundé region from the Neoprotorezoic Pan-African belt in southern Cameroon (Central Africa). *Journal of African Earth Sciences,* 44: 443–458.

Štelcl, J. & Svoboda, L., 1962. Petrografické studie kulmských sedimentů Drahanské vysočiny (těžké minerály kulmských drob). *Folia Universitatis Purkynianae Brunensis, Geologia*, 3: 1–50. [In Czech.]

Triebold, S., von Eynatten, H. & Zack, T., 2005. Trace elements in detrital rutile as provenance indicators: a case study from the Erzgebirge, Germany. *Schriftenreihe der Deutschen Gesellschaft für Geowissenschaften*, 38: 44–145.

Tucker, M. (ed.), 1988. *Techniques in Sedimentology*. Blackwell Science, Oxford, 394 pp.

Vysloužil, O., 1981. *Fauna spodního badenu na lokalitě Služín v karpatské předhlubní na Moravě*. Unpublished MSc Thesis, Masaryk University, Brno. [In Czech.]

Walker, R. G. & James, N. P., 1992. *Facies Models: Response to Sea Level Changes.* Geological Association of Canada, St. John's, 380 pp.

Zack, T., von Eynatten, H. & Kronz, A., 2004. Rutile geochemistry and its potential use in quantitative provenance studies. *Sedimentary Geology*, 171: 37–58.

Zapletal, J., 2004. Contribution to paleogeographic evolution of Lower Bedenian sedimentation in central Moravia (Czech Republic). *Scripta Facultatis Scientiarum Naturalium Universitatis Masarykianae Brunensis, Geology,* 31–32: 87–98. [In Czech.]

Zapletal, J., Hladilová, Š. & Doláková, N., 2001. Marine sediments of the Lower Badenian marginal facies in Olomouc. *Scripta Facultatis Scientiarum Naturalium Universitatis Masarykianae Brunensis, Geology,* 30: 75–86. [In Czech].

Zágoršek, K., 2010. Bryozoa from the Langhian (Miocene) of the Czech Republic. Part I and II. *Acta Musei Nationalis Pragae, Series B, Historia Naturalis*, 66: 1–255.

Zágoršek, K., Holcová, K., Nehyba, S., Kroh, A. & Hladilová, Š., 2009. The invertebrate fauna of the Middle Miocene (Lower Badenian) sediments of Kralice nad Oslavou (Central Paratethys, Moravian part of the Carpathian Foredeep). *Bulletin of Geosciences*, 84: 465–496.

Zágoršek, K., Nehyba, S., Tomanová Petrová, P., Hladilová, Š., Bitner, M. A., Doláková, N., Hrabovský, J. & Jašková, V., 2012. Local catastrophe near Přemyslovice (Moravia, Czech Republic) during Middle Miocene due to the tephra input. *Geological Quarterly*, 56: 269–284.

Zágoršek, K., Tomanová Petrová, P., Nehyba, S., Jašková, V. & Hladilová, Š., 2010. Fauna vrtů HL 1a HL 2 u Hluchova (střední miocén), Prostějovsko. *Geologické výzkumy na Moravě a ve Slezsku v roce 2009*, 17: 99–103.